COMPUTER SIMULATION OF GAS-SURFACE INTERACTIONS USING THE LENNARD-JONES POTENTIAL FUNCTION

A THESIS

Presented to

The Faculty of the Division of Graduate

Studies and Research

by

Rand Hampton Childs

In Partial Fulfillment

of the Requirements for the Degree

Master of Science in Chemistry

Georgia Institute of Technology

April, 1977

COMPUTER SIMULATION OF GAS-SURFACE INTERACTIONS

USING THE LENNARD-JONES POTENTIAL FUNCTION

Approved:

Peter B. Sherry, Chairman

Robert A. Pierotti

Arlon P. Jensen

Date approved by Chairman 19th April 1977

ACKNOWLEDGMENTS

I would like to thank my thesis advisor, Dr. Peter Sherry, for his advice and assistance during the course of this work. The help that Spotswood Stoddard gave me during the development of the computer model is greatly appreciated. I would also like to thank the Graduate Division for waiving certain requirements so that this thesis could be produced using a computerized text processing system.

I would like to extend my sincere appreciation to my close friend and fellow mapmaker. His encourgement and support has helped me for many years and I am truly greatful, Mapmaker, many thanks for the help that you have given me with my map.

TABLE OF CONTENTS

		Page
ACKNOWLEDGMENTS		ii
LIST OF TABLES		iv
LIST OF ILLUSTRATIONS		v
SUMMARY		vi
Chapter		
I.	INTRODUCTION	1
II.	HISTORICAL	4
III.	THEORETICAL	15
IV.	THE COMPUTER MODEL	29
V.	RESULTS AND CONCLUSIONS	53
BIBLIOGRAPHY		80

LIST OF TABLES

Table		Page
1.	Conversion Between Computer Units and CGS Units	60
2.	Numerical Conversion Factors Between Computer Units and CGS Units for Various Inert Monatomic Gases	61
3.	Numerical Results of the 12 NOWALL Experiments in Computer Units	66
4.	Numerical Results of the 13 WALL Experiments in Computer Units	67
5.	Numerical Values of the Theoretical and Experimental Second Virial Coefficient at Various Values of Temperature for the NOWALL Model	69
6.	Numerical Values of the Theoretical and Experimental Second Virial Coefficient at Various Values of Temperature for the WALL Model	70
7.	Numerical Values for the Number of Particles Adsorbed and the Change in Enthalpy for Various Values of Temperature for the WALL Model	75
8.	Numerical Values of the Temperature and the Second Gas-Solid Virial Coefficient in Computer Units	77

LIST OF ILLUSTRATIONS

Figure		Page
1.	Plot of the Reduced Lennard-Jones 6-12 Potential Function	18
2.	The NOWALL Model	23
3.	The WALL Model	26
4.	The Routines Composing the NOWALL and WALL Models	33
5.	The Main Driver Routine	35
6.	The Routine IPT	38
7.	The Routine INSET	39
8.	The Routine EA	41
9.	The Routine RK	48
10.	A Circular List L_i	50
11.	Possible Intersections of the O_i and L_i Lists	50
12.	The Routine CHIS	52
13.	Plot of the Motion of 20 Particles Using the WALL Model	57
13A.	Plot of the Motion of 20 Particles Using the WALL Model	58
14.	Plot of the Theoretical Second Virial Coefficients with the Experimental Second Virial Coefficients Calculated Using the WALL and NOWALL Models	71

SUMMARY

Two computer models were developed to simulate gas-surface interactions using a Lennard-Jones 6-12 potential function. The first computer model, the NOWALL model, calculates the molecular dynamics of a dilute classical Lennard-Jones gas in a box with cyclic boundary conditions. The second model, the WALL model, calculates the molecular dynamics of a dilute classical Lennard-Jones gas in a box whose walls consist of rigid particles interacting with the gas through a Lennard-Jones potential function. From equilibrium pressure and temperature data, experimental second virial coefficients were calculated for both systems. Experimental second virial coefficients calculated from the NOWALL model agree reasonably well with theoretical values over the entire temperature range. Experimental second virial coefficients calculated from the WALL model deviate negatively from the theoretical second virial coefficients at low temperature, indicating that some of the particles in the system have been adsorbed on the wall. The number of particles adsorbed, the second gas-solid virial coefficient, and the enthalpy of adsorption were computed. The data indicates that the heat of adsorption, ΔH_{ads}, calculated from the WALL model is approximately one tenth that of

experimental values for a real gas. Although it is not surprising that the WALL model is insufficient to calculate numerical quantities such as ΔH_{ads} for the adsorption of a gas on a wall with great accuracy, the model is sufficient to indicate trends in such quantities, and also accurately predicts that adsorption occurs at low temperature.

CHAPTER I

INTRODUCTION

The molecular dynamics approach to modeling a system of inert monatomic gas particles has existed for approximately 20 years. Much of the research in the field was performed using hard sphere or square-well interaction potentials to calculate the dynamic motion of particles in dense gases, liquids, or solids. A few researchers extended these calculations to include a Lennard-Jones interaction potential, although these studies were made primarily for dense particle systems. Molecular dynamics calculations of dilute gaseous systems were begun in 1971 when Harrison and Schieve (1) reported their study of a dilute two-dimensional gas system. An extention of this type of research would be to model dilute gaseous systems using the technique of molecular dynamics, expecially in the area of gas-surface interactions.

This research is primarily concerned with the possibility of modeling gas-surface interactions using the Lennard-Jones potential function. This can be accomplished by modeling a gas in the absence and presence of a wall and

comparing results of each model.

Two computer models were developed. The first model consists of a dilute monatomic Lennard-Jones gas in a box with cyclic boundary conditions. The second model consists of a dilute monatomic Lennard-Jones gas in a rigid box whose walls are composed of particles of the same diameter as the particles in the gas and aligned along the boundary of the box. In addition, a Lennard-Jones potential exists between the gas particles and the particles along the wall.

By performing computer simulations of each model at low temperatures, the equilibrium temperature and pressure may be determined, and from this data an experimental second virial coefficient may be calculated for each system. Comparison of the experimental second virial coefficients with theoretical values allows a determination of the effect of the wall on the gaseous system. In particular, adsorption of gas molecules on the wall due to the gas-surface interaction may be observed.

This thesis consists of five chapters and a bibliography. Chapter II outlines the historical development of molecular dynamics calculations. Chapter III develops the theoretical equations that must be solved to determine the position and momentum of a particle as a function of time.

The third chapter concludes with a description of the two computer models. Chapter IV discusses the advantages and disadvantages of computer programs developed by other researchers, and describes the algorithms used in the computer model developed for this research. Chapter V gives the results and conclusions of the molecular dynamics experiments performed using the two computer models.

The computer models were written in Control Data Corporation Extended FORTRAN. The numerical results reported in this research were calculated using a Control Data Corporation CYBER 74-28 computer system at the Office of Computing Services, Georgia Institute of Technology.

CHAPTER II

HISTORICAL

In the present age of numerous high speed multiprocessing and multiprogramming computer systems with arrays of sophisticated compilers and operating systems, it is difficult to conceive of the enormous problems that must have confronted scientists interested in computer modeling in the mid 1950's. Despite computer hardware and software limitations, the work of B. J. Alder and T. E. Wainwright during the late 1950's and early 1960's pioneered the development of molecular dynamics calculations.

In 1957 Alder and Wainwright (2), in a letter to the editor, described briefly the design of "a calculation of molecular dynamic motion". Using electronic computers they solved the simultaneous classical equations of motion for systems of 32 and 108 particles initially placed in an ordered lattice in a rectangular box with periodic boundry conditions. The particles were given initial velocities of equal magnitude but random orientations. After a short initial run, the system reached the Maxwell-Boltzmann velocity distribution. The surprising result of their

initial investigation was the observation that the pressure of the system jumped suddenly from one level to another as their calculation proceeded. Their hard sphere molecular model had exhibited a phase transition.

Not long after their original publication, Alder and Wainwright published two more papers developing their methods and extending their calculations. Their second paper (3), published in 1958, modeled hard sphere periodic particle systems ranging in number from 32 to 500. Most of their work was done in the high density fluid or solid region. They discussed the Boltzmann H-function and indicated that over a wide range of densities, the equilibrium value for a hard sphere system is reached monotonically in two to four collisions per particle. They compared the collision rate for both a 32 and 108 particle system with that given by the kinetic theory of Enskog and found excellent agreement. Finally, they discussed the phase transitions observed between solid and fluid states over a narrow range of densities. Pictures were presented, produced from a cathode ray tube attached to the computer, of the traces in a plane projection of the positions of the centers of the particles in a 32 particle hard sphere system. These pictures, along with tabulated data, clearly indicated solid-fluid phase transitions. In their third paper (4), and the first in a series of studies in molecular dynamics, Alder and Wainwright

outlined in great detail their method for studing the many-body problem with an electronic computer. They included a flowchart of the logical sequence of the calculations and discussed an algorithm for the solution of a molecular dynamics problem using the square-well potential. Limitations of the numerical scheme were enumerated, and the important steps necessary to make the program efficient were indicated. In 1960 Alder and Wainwright (5) reported the results of a molecular dynamics calculation of the equation of state and collision rate for hard sphere systems ranging in size from four to 500 particles. They qualitatively discussed the dependence of the results on the number of particles, and compared the results to various analytical theories. Earlier they reported (3) that it might be possible for a fluid and solid state to coexist in a many particle system. However, they determined that systems as large as 500 particles were insufficient for the coexistence of the two states. A comparison of the collision rate for many different multi-particle systems with the Enskog theory for the collision rate gave excellent agreement over a wide density region. The authors calculated and presented the equation of state for hard body systems ranging in size from four to 500 particles and ranging in density from a dense gas to a solid. A comparison of these results with the superposition and free-volume theories established that the free-volume theory was only valid in the high density solid

region, and the superposition theory was only valid in the lower density dense-gas region. Finally the authors concluded that hard sphere systems as small as 100 particles were sufficient to describe accurately the equilibrium behavior in the fluid region.

The work of Alder and Wainwright inspired others to model dense fluid systems using the technique of molecular dynamics. Aneesur Rahman, of the Argonne National Laboratory, made significant contributions to the field. Whereas Alder had chosen the hard sphere 2-body potential for his model, Rahman chose the more realistic Lennard-Jones 6-12 2-body potential. In 1964 Rahman (6) published the results of the first simulation of a liquid whose particles were interacting through a Lennard-Jones potential. His system consisted of 864 particles at 94.4 degrees Kelvin placed in a cubical box with periodic boundry conditions (4). The Lennard-Jones ε and σ and the mass were chosen to simulate argon. His studies of the pair correlation function and the self diffusion coefficient agreed well with experimental results. Rahman's approach was significant since his work represented the first attempt to identify a molecular dynamics system with a physical system.

An interesting comparison can be made of molecular dynamics results using two distinctly different 2-body

interaction potentials. In separate studies, Alder (7) and Rahman (8) compared the superposition approximation with a numerical computation of the pair and triplet distribution functions of dense liquids. Alder indicated that the pair distribution function calculated from the Born-Green integral equation lead to large errors when compared with the pair distribution function calculated from molecular dynamics. Rahman, however, indicated that if the more realistic Lennard-Jones model was used, the Born-Green pair distribution function did not seem to be any worse than the molecular dynamics pair distribution function.

In another paper published in 1964, Alder (9) continued his comparison of theory with molecular dynamics computer experiments. He was interested in the theory of mixing, and developed a molecular dynamics experiment consisting of an equimolar mixture of 500 hard spheres differing in radius by a factor of three. Comparison of the molecular dynamics equation of state and the change in pressure upon mixing at fluid density with the compressibility and virial equation of state of the Percus-Yevick theory of mixing gave some indication of the relative value of the two forms of the theory. In both cases the numerical solution was bounded by the two versions of the theory and was in better agreement with the compressibility equation. This indicated that the compressibility form of

the Percus-Yevick theory was more accurate than the virial equation of state. Alder also determined that the excess volume, entropy, and free energy upon mixing at constant pressure were extraordinarily small considering the enormous difference in the size of the particles. Alder concluded that in mixing of ordinary liquids, the difference in size of the molecule is of less importance than the interaction potential in determining excess properties.

The success of earlier molecular dynamics computer experiments lead to numerous studies of hard sphere, dense fluid systems by Alder and co-workers during the next five years. In 1966 Alder and Dymond (10) developed a theory of transport properties based on the van der Waals concept of a dense fluid. Molecular dynamics calculations of rare gas transport coefficients at temperatures and densities greater than the critical values agreed to within 10% of experimental results. Alder and Wainwright (11), in 1967, made a comprehensive study of the velocity autocorrelation function for hard spheres over the entire fluid density range. They found that deviations from exponential behavior were small. In 1970 Alder, Gass, and Wainwright (12) published their results of a molecular dynamics calculation of the transport coefficients for a hard sphere fluid. The diffusion coefficient, the shear and bulk viscosity, and the thermal conductivity were evaluated by means of their

Einstein expressions over most of the fluid region. The results are given for systems of 108 particles, but a few systems of 500 particles were presented as well. Comparisons were made with the Enskog theory. The largest deviations of the transport coefficients occured near solid densities. The viscosity was about twice as large as the Enskog prediction and the diffusion coefficient was about a factor of two smaller. Deviations from the Enskog theory for the thermal conductivity and bulk viscosity were barely perceptible within the few percent accuracy of the data.

It is important to know how well a particular interaction potential will model a physical system. In 1967, Loup Verlet (13) published the results of a molecular dynamics calculation of the thermodynamical properties of Lennard-Jones molecules. His system consisted of 864 particles enclosed in a cube with periodic boundary conditions. The value of ε and σ were chosen for argon. The equilibrium thermodynamic properties were calculated at various values of the temperature and density, relative, generally, to a fluid state. The striking result of this study was the over-all agreement between the molecular dynamics results and the thermodynamics of real argon. Verlet (14) also published a review of the various phase transitions observed with the aid of fast electronic computers in 1969, and a year later he published another

review (15) of computer calculations on classical fluids.

During the late 1960's, Rahman turned his attention to modeling solids via molecular dynamics. In 1969, Allen, DeWette, and Rahman (16) reported the results of a calculation of various surface properties of noble gas crystals. All calculations were performed for a Lennard-Jones pair-potential. The results of the molecular dynamics calculations were compared with those obtained by Allen and DeWette (17) through lattice dynamics in the quasiharmonic approximation. The results for the displacement of the mean atomic positions (from positions in the bulk) agreed well with those found through lattice dynamics. The results for the mean square amplitudes agreed well for atoms a few layers beneath the surface, but indicated that anharmonicity caused a substantial increase in these quantities near the surface. Also that year DeWette, Allen, Hughes, and Rahman (18) reported that they had obtained crystallization of a two-dimensional system of particles interacting through a Lennard-Jones potential. The two-dimensional system consisted of 400 particles. Crystallization resulted entirely from the interaction of the particles; i. e., there were neither walls enclosing the system nor periodic boundary conditions. In a third paper published in 1969, Rahman (19) restated the problem of molecular dynamics, and reviewed much of his previous work on

condensed systems. He also discussed some preliminary molecular dynamics calculations of the pair correlation function of a system of 1024 electrons.

Although Alder had done extensive calculations on dense systems using the hard sphere and square-well potentials, and Rahman and Verlet had studied the properties of liquid and solid systems, using the more realistic Lennard-Jones potential, it was not until 1971 that a study of a dilute gas system was reported. Harrision and Schieve (1) reported on a molecular dynamics calculation of a dilute gas system of 100 particles interacting through a Lennard-Jones 6-12 potential. Two calculations were performed for the Boltzmann H-function. One calculation was restricted to the repulsive part of the Lennard-Jones potential. It was found that equilibrium for the Lennard-Jones repulsive core was achieved in two to three collisions per particle, in agreement with the Alder-Wainwright results (3). When the attractive tail was added, the H-function decreased more rapidly and the particles made four to five collisions per particle in the same amount of time. Continuing with their work, Harrision, Schieve, and Turner (20) observed the formation and dissociation of classical bound pairs (dimers) in a molecular dynamics calculation for two-dimensional dilute argon gas consisting of 100 particles. In another study by Harrision

and Schieve (21), the dimer mole fraction was determined for nine systems with different temperatures and densities. Their results were found to agree with the theoretical dependences predicted by Stogryn and Hirschfelder. These results were also shown to be consistant with experimental measurements.

Recent molecular dynamics studies have been numerous and quite varied. Borstnik (22) studied the velocity distribution function, pair correlation function, diffusion constants, and velocity autocorrelation function for a three-dimension two-component Lennard-Jones mixture. Alder and co-workers studied the vacancy motion in hard sphere crystals (23), the thermal conductivity of a hard sphere solid (24), the square-well fluid (25), and the velocity autocorrelation function of a hard sphere solute particle of the same size but different mass from the solvent particles (26) and compared and reviewed the Monte Carlo and molecular dynamics methods (27). Rahman and Stillinger, using molecular dynamics, studied a dynamical model of liquid water (28), the temperature effects on water structure and kinetics (29), and a molecular dynamics calculation of molecular motion in water (30). Both Alder and co-workers (31, 32) and Rahman and co-workers (33) studied depolarized light scattering from monatomic fluids using the techniques of molecular dynamics. Finally, Subramanina, Levitt, and Davis

(34) recently made computer studies of the onset of Brownian motion in a hard sphere fluid.

In 1973 Schofield (35) published a review with eight references on computer simulation of molecular dynamics in liquids and its application for the calculation of the effect of the attractive part of the Lennard-Jones potential in liquids, the self-diffusion coefficients of liquids as a function of temperature and density, and as a function of various interparticle potentials, and the equation of state and pair distribution functions for liquids with different repulsive potentials.

A complete review of the entire subject of molecular dynamics was published by Alder (36) in 1973. Much of his own work is reviewed carefully for the first time. This review has an extensive bibliography with 48 entries.

CHAPTER III

THEORETICAL

In order to develop a mathematical model of an inert monatomic gas system, a suitable potential function must be choosen. The Lennard-Jones 6-12 pair potential was selected for this work as best representing the interaction between two inert gas molecules within the limitations imposed by computer time and the mechanics of the problem, thus only 2-body interactions will be accounted for.

The Lennard-Jones potential is given by

$$U(r) = 4\varepsilon[-(\frac{\sigma}{r})^6 + (\frac{\sigma}{r})^{12}] \qquad (1)$$

where r is the distance between two particles and ε and σ are parameters dependent upon the particular gas molecule to be studied.

Equation (1) was modified slightly to have a finite range in the computer calculations. Given a finite range r_c of the interaction, equation (1) can be rewriten as

$$U(r) = 4\epsilon[(\frac{\sigma}{r})^{12} - (\frac{\sigma}{r})^{6} + (6(\frac{\sigma}{r_c})^{12} - 3(\frac{\sigma}{r_c})^{6})(\frac{r}{r_c})^{2} - 7(\frac{\sigma}{r_c})^{12} + 4(\frac{\sigma}{r_c})^{6}] \quad (2)$$

such that $U(r)$ approaches zero as r approaches r_c. It is assumed that $U(r)$ equals zero for $r \geq r_c$. In order to prevent a discontinuity, which might cause computational problems, $U(r)$ of equation (2) and its first derivative $dU(r)/dr$ go continuously to zero as r approaches r_c. Equations (1) and (2) differ only slightly when r_c is taken to be several times the size of σ. This form of the Lennard-Jones potential was first used by Stoddard (38).

It is convenient to express equation (2) in terms of a reduced system of units. Distance can be expressed in units of σ, energy in units of 4ϵ, and mass in units of m.

Let $r' = r/\sigma$, therefore $r_c' = r_c/\sigma$ and dropping the primes, equation (2) becomes in reduced coordinates

$$U(r) = 4\epsilon[\frac{1}{r^{12}} - \frac{1}{r^{6}} + (\frac{6}{r_c^{12}} - \frac{3}{r_c^{6}})(\frac{r}{r_c})^{2} - \frac{7}{r_c^{12}} + \frac{4}{r_c^{6}}] .$$

Let $U'(r') = U(r')/4\epsilon$, and again dropping the primes the reduced potential function becomes

$$U(r) = \frac{1}{r^{12}} - \frac{1}{r^{6}} + (\frac{6}{r_c^{12}} - \frac{3}{r_c^{6}})(\frac{r}{r_c})^{2} - \frac{7}{r_c^{12}} + \frac{4}{r_c^{6}} . \quad (3)$$

This reduced potential function, as used in the computer experiments, is plotted in Figure 1.

The force acting on particle i due to particle j is equal to the negative of the first derivative of the potential with respect to position, or

$$F(r) = - \frac{dU(r)}{dr} \tag{4}$$

where the distance r between particles i and j is given by

$$r = |\vec{r}_i - \vec{r}_j| \quad . \tag{5}$$

The force function, equation (4), can now be equated to Newton's second law, $F = m\ddot{r}$, giving

$$m\ddot{r} = - \frac{dU(r)}{dr} \quad . \tag{6}$$

Since equation (6) is a time dependent equation, time should also be expressed in reduced units. Equating the negative of the first derivative of equation (2) to Newton's second law gives

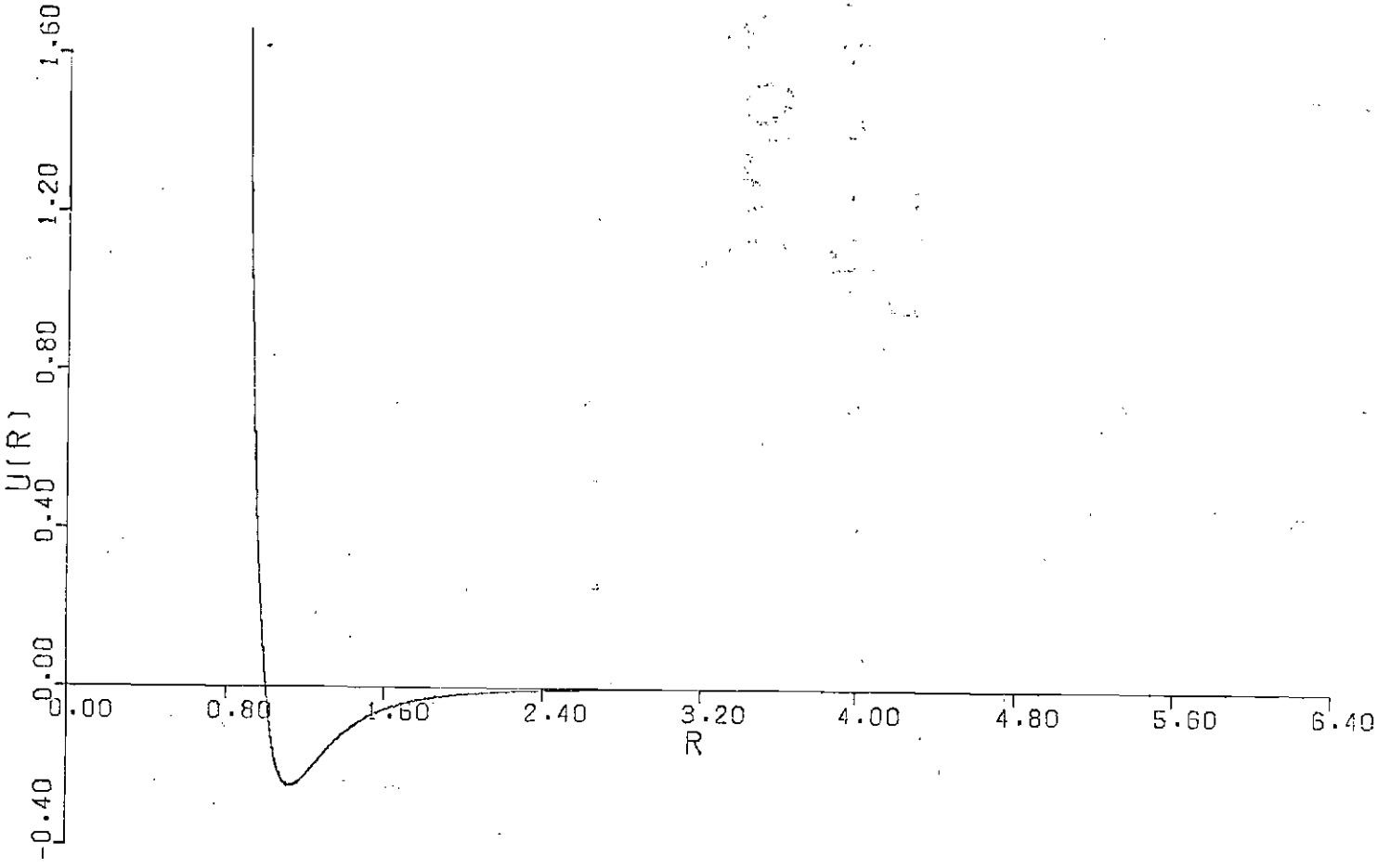

Figure 1. Plot of the Reduced Lennard-Jones 6-12 Potential Function.

$$\frac{md^2r}{dt^2} = -\frac{dU}{dr} \quad . \qquad (7)$$

Again using primes for reduced coordinates

$$\frac{dU}{dr'} = \frac{dU}{dr}\frac{dr}{dr'} = \frac{dU}{dr}\sigma$$

then equation (7) becomes

$$m\frac{d^2r}{dt^2} = -\frac{1}{\sigma}\frac{dU}{dr'} \quad . \qquad (8)$$

Given that

$$\frac{d^2r}{dt^2} = \sigma\frac{d^2r'}{dt^2}$$

equation (8) becomes

$$m\sigma\frac{d^2r'}{dt^2} = -\frac{1}{\sigma}\frac{dU}{dr'} \qquad (9)$$

and since

$$U' = \frac{U}{4\varepsilon}$$

equation (9) may be rewriten as

$$m\sigma^2 \frac{d^2r'}{dt^2} = - 4\varepsilon \frac{dU'}{dr'} \quad . \tag{10}$$

Given equation (10), a reduced time can be defined as

$$t' = \frac{t}{(\frac{m\sigma^2}{4\varepsilon})^{1/2}} \quad .$$

Equation (10) then becomes

$$\frac{d^2r'}{dt'^2} = - \frac{dU'}{dr'} \quad . \tag{11}$$

Equation (6), the equation of motion for particle i can now be rewriten in reduced units, omitting the primes, as

$$\frac{d^2r}{dt^2} = - \frac{dU}{dr} \quad . \tag{12}$$

For a N particle system, the time dependent second order differential equation of motion for particle i,

equation (12), becomes

$$\frac{d^2 r_i}{dt^2} = \sum_{\substack{i=1 \\ j \neq i}}^{N} - \frac{dU(r_{ij})}{dr_{ij}} \qquad (13)$$

where r_i is the position of particle i and r_{ij} is the distance between particles i and j.

To describe the motion of each of the N particles in a gaseous system with 2-body interactions, it is necessary to solve N such equations of the form of equation (13). There being no exact solution for r as a function of t, a numerical approximation method must be chosen to obtain an approximate solution for the position and momentum of the N particles in the system. A Runge-Kutta integration procedure is used in this work to solve the appropriate set of differential equations obtained from equation (13). A description of the procedure is given in Chapter IV.

The solution of this set of equations for momentum and position leads to the calculation of a reduced temperature for the system. The reduced temperature T is calculated as the time average of the instantaneous temperature defined by

$$T = \frac{1}{Nk} \sum_{i=1}^{N} \frac{1}{2} m v_i \qquad (14)$$

where v_i is the reduced velocity of the ith particle, m is the reduced mass, and k is the reduced Boltzmann constant which is equal to 1.

Since this work is concerned with the effect of a wall on the second virial coefficient, it is necessary to describe the Lennard-Jones gas under two different conditions; 1) contained in a box with walls, and 2) contained in a box with no walls (cyclic boundary). Any effect due to the wall may be observed by computing the second virial coefficients from the equilibrium pressure and temperature for both systems.

The first model, which is called the NOWALL model, consists of N particles in a two-dimensional square box with cyclic boundary conditions. Under such a boundary condition, particles interact cyclically through the walls of the box and a particle which passes out of one side of the box reenters through the opposite side of the box with the same momentum and direction. Figure 2 illustrates the NOWALL model. From the kinetic theory of gases, each time a particle passes through the wall it imparts a momentum of $2mv_{ci}$ to the wall, where v_{ci} is the component of the velocity of particle i normal to the wall. The total momentum imparted to the walls after some time t would be the sum of

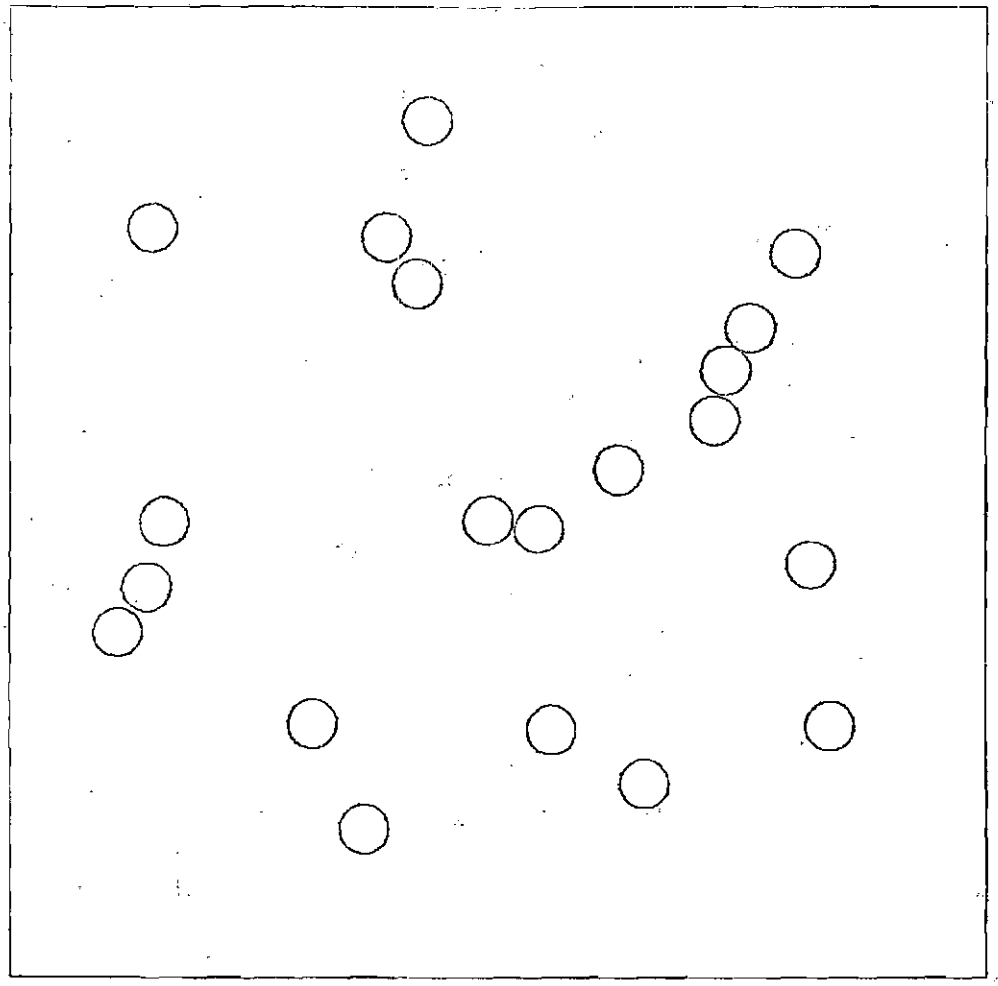

Figure 2. The NOWALL Model.

all contributions of $2mv_{ci}$ due to collisions with the walls by the N particles in the box. This may be represented by

$$\rho_t = \sum_{t=0}^{t} 2mv_{ci} \quad .$$

The total rate of transfer of momentum, that is, the total force on the walls at time t is then

$$F_t = \frac{\rho_t}{t}$$

and the pressure in the box at time t is the force on the walls divided by the area of the walls, A, or

$$P_t = \frac{F_t}{A} \quad . \tag{15}$$

Equation (15) is used to calculate the pressure of the NOWALL model system at any time t.

The second model, which is called the WALL model, was designed to approximate a Lennard-Jones gas bounded by a wall. It consists of N particles in a two-dimensional square box. The walls of this box are composed of particles which are the same diameter as particles in the gas and are aligned along the boundary of the box. These wall particles interact

with the gas particles through the same Lennard-Jones potential that exists between the particles of the gas. The wall particles are considered fixed in space so that no momentum is exchanged during a collision between a gas particle and the wall. Figure 3 illustrates the WALL model.

For such a system both the gas particle-gas particle interaction and the wall particle-wall particle interaction must be considered. Therefore, for a N particle system with W wall particles, the time dependent second order differential equation of motion for particle i becomes

$$\frac{d^2 r_i}{dt^2} = \sum_{\substack{j=1 \\ j \neq i}}^{N} - \frac{dU(r_{ij})}{dr_{ij}} + \sum_{k=1}^{W} - \frac{dU(r_{ik})}{dr_{ik}} \qquad (16)$$

where r_i is the position of particle i and r_{ij} is the distance between particles i and j.

From equation (4), the momentum change due to the N particles interacting with the wall particles after some infinitesimal time dt is just

$$\rho_{dt} = \sum_{i=1}^{N} \sum_{k=1}^{W} - \left. \frac{dU(r_{ik})}{dr_{ik}} \right|_{\perp} dt$$

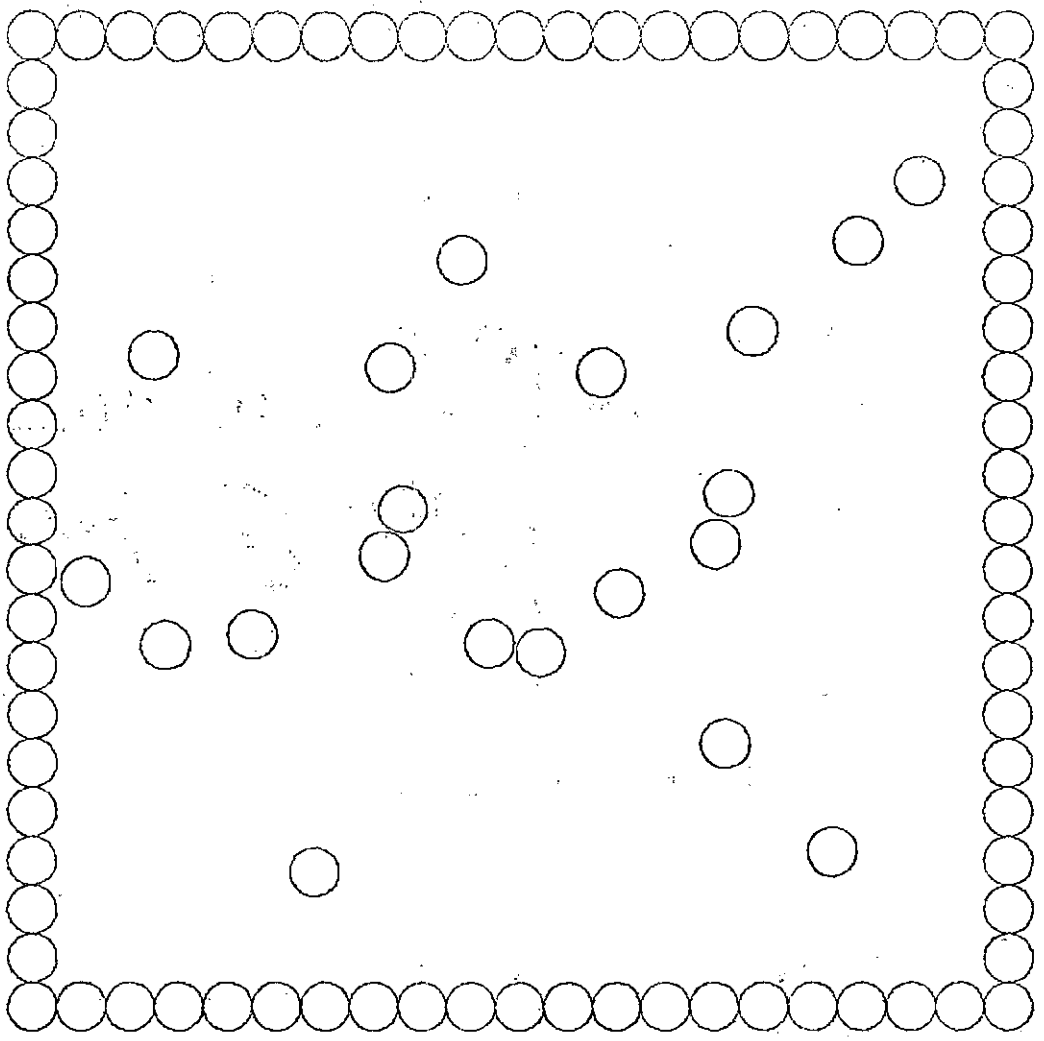

Figure 3, The WALL Model.

where

$$- \left. \frac{dU(r_{ik})}{dr_{ik}} \right|_{\perp}$$

is the component of the force normal to the wall. The total momentum change after time t becomes

$$\rho_t = \int_0^t \sum_{i=1}^{N} \sum_{k=1}^{W} - \left. \frac{dU(r_{ik})}{dr_{ik}} \right|_{\perp} dt \quad .$$

Therefore the total rate of change of momentum, that is, the total force on the walls due to the interaction of the wall particles with the gas particles at time t is given by

$$F_t = \frac{\rho_t}{t} \quad . \tag{17}$$

As before, the pressure at any time t is the force, equation (17), divided by the area of the walls, A, or

$$P_t = \frac{F_t}{A} \quad . \tag{18}$$

The NOWALL model and the WALL model are identical except for their boundary conditions. The pressure,

temperature, and the second virial coefficient may be calculated for either system, and a determination of the effect of a wall may be made.

CHAPTER IV

THE COMPUTER MODEL

The computer molecular dynamics calculations are divided into two main groups. One group, represented by the works of Alder and Wainwright, deals with systems of hard sphere or square-well potential functions. The second group, represented by the works of Rahman and collaborators, deals with more realistic potential functions, such as the Lennard-Jones 6-12 potential function, to describe a molecular dynamics system of interacting particles.

The hard sphere model chosen by Alder and Wainwright (4) had the advantage of computational simplicity and speed. The force acting on each of the particles in the system is either constant or zero for short time intervals during which the particles are allowed to move. Under such conditions, a computer program does not have to deal with the problems of integrating repulsive or attractive interactions where the forces on the particles change very rapidly.

In hard sphere calculations, the successive molecular positions were calculated by straight line trajectories

except during a collision. Alder and Wainwright developed an algorithm to determine the time at which a collision between two particles would occur. For that time the velocity changes were calculated from simple conservation laws, and no integration of Newton's equations of motion was necessary. Since any numerical integration on a digital computer is, by its nature, very time consuming, this choice of potential function saved Alder and Wainwright computer time. It must be pointed out, however, neither the hard sphere potential nor the square-well potential may be as realistic as other potential functions for modeling gaseous systems.

Rahman (6) recognized the limitations of the hard sphere model and developed a computer model to solve the classical equations of motion for a system of particles interacting with a Lennard-Jones potential function. His solution was to solve numerically the 6N differential equations of motion arising from Newton's law. The differential equations were solved using a set of difference equations with a time increment of 10^{-14} seconds. The advantage of this technique is that it can be applied not only to the Lennard-Jones but to other potential functions as well, and is independent of the density of the system. The only requirement is that the time increment for the integration procedure be small enough for the integration procedure to yield new positions and velocities within an

acceptable truncation error.

The major drawback of the Rahman technique is the fixed time increment. It must be small enough to predict correctly the new positions and velocities of two interacting particles, but may be too small for particles that are not interacting with other particles in the system. Rahman's technique would work well for moderate and high density systems but would waste computer time for dilute gas systems.

Recently two separate works have appeared which combine the Alder-Wainwright algorithm and the Rahman technique to improve the computational efficiency for the solution of the molecular dynamics of a dilute gas. Harrision and Schieve (1) used the Alder-Wainwright technique for the description of the molecular trajectories of non-interacting particles with the Rahman method to solve the equations of motion of interacting particles. Aharony (37) used a modified Alder-Wainwright algorithm between collisions, making use of the conservations laws in the binary case.

The computer program developed for the purpose of this research was a modification of a program developed by Stoddard (38). The program was designed with several irportant prerequisities in mind. The program was written in

a modular fashion with a small main driving program to call logically independent subroutines which perform the major calculations and input-output. One advantage of this technique is greater ease of debugging, since a short main driver can be written to call any one of the subroutines. If known data is used as input results can be verified. Also this technique allows additional flexibility if it becomes necessary to add additional capabilities to the program. In most instances each modification can be incorporated as an additional module. Figure 4 illustrates the main driver and each of the different subroutines.

It was important that the program perform the computations with a high degree of accuracy, that it be rather efficient for dilute as well as for dense gaseous systems, and that no assumptions be made as to the "state of a collision". For this reason, the Rahman technique (6) was used to solve the equations of motion, but an integration scheme was developed which did not use a fixed time increment so that the efficiency of the program would be improved.

The amount of computer time that one can obtain for any particular computer experiment is necessarily limited. Therefore, after a predetermined amount of central processor time has been utilized, the program will store all of the data that are necessary for a restart at some later time, and

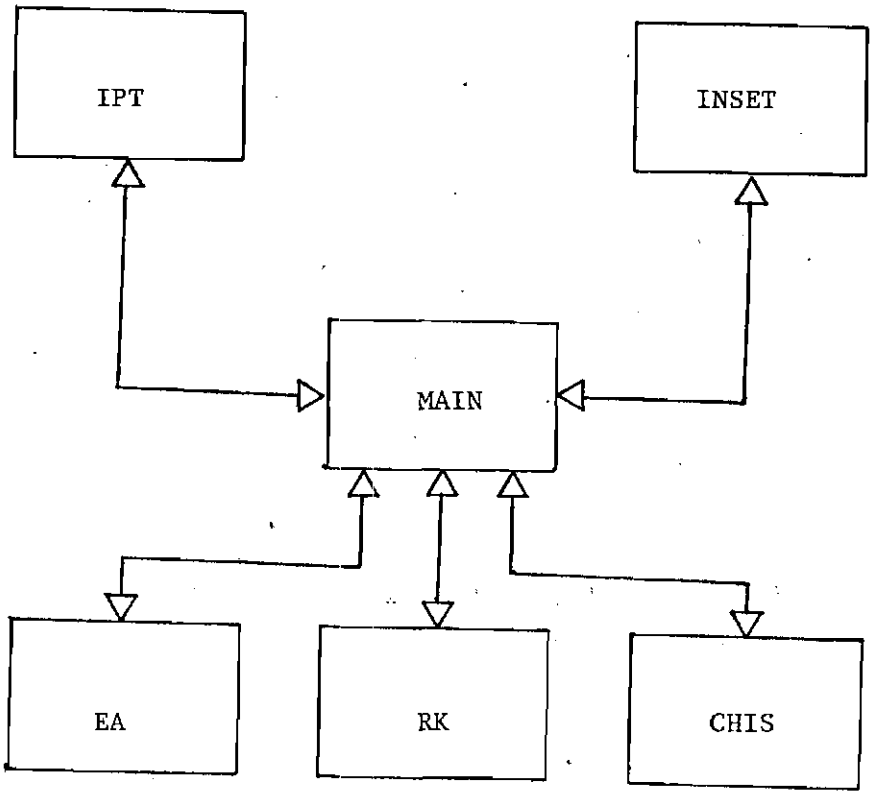

Figure 4. The Routines Composing the NOWALL and WALL Models.

then stop.

The program is composed of the routines MAIN, IPT, INSET, EA, CHIS, and RK. Each of these routines will be described in some further detail.

MAIN

MAIN is the main driver program which calls each of the other routines. It also checks the amount of central processor time used by the program and compares this with a maximum value read in as data thru IPT. If the time used is within one minute of the maximum allowed, MAIN will call the appropriate routine to checkpoint (output the restart data) and then stop program execution. Figure 5 illustrates the logic of MAIN.

IPT

IPT is the routine which performs all input and output for the program. From the input data, IPT determines if this run is an initial computer experiment or a continuation of a previous run. If the run is the beginning of an experiment, IPT will input the number of particles, either the size of the box or the density, the initial temperature of the

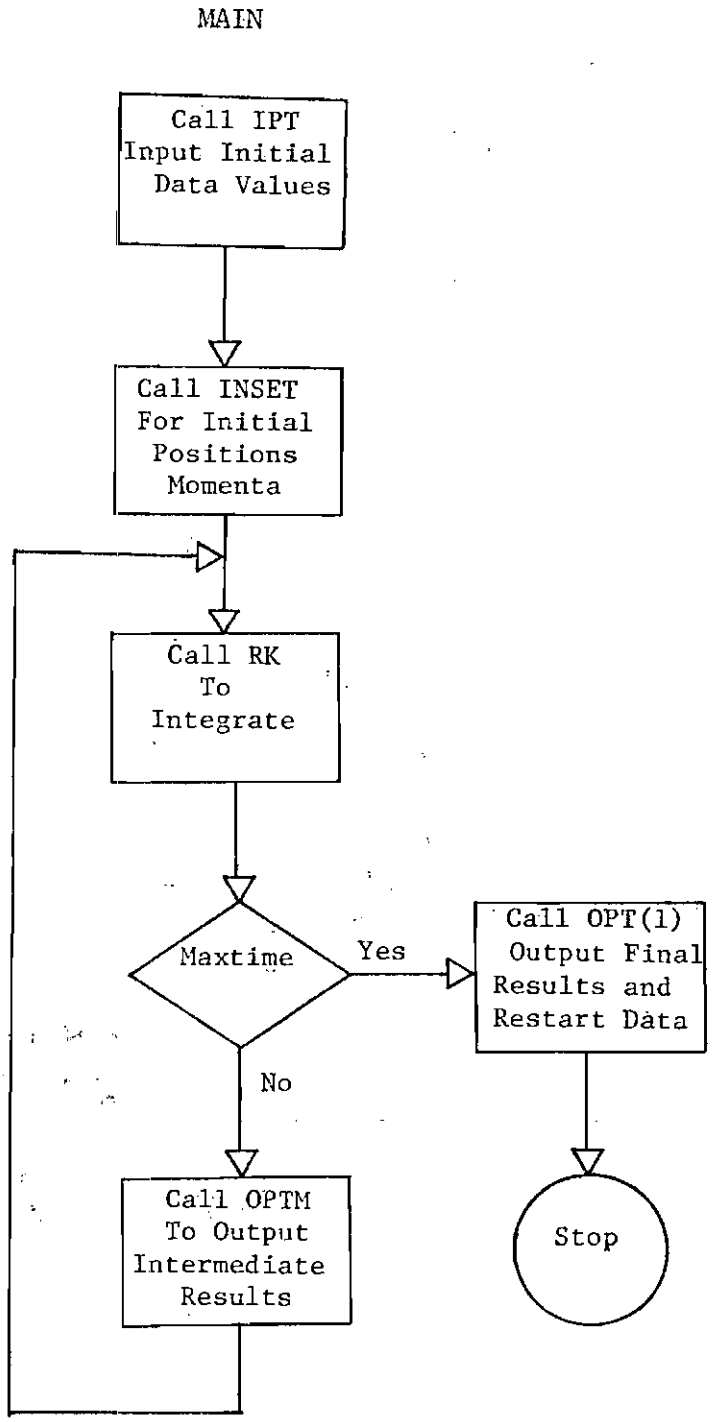

Figure 5. The Main Driver Routine.

system, the dimension of the system (either two or three), and the maximum amount of central processor time that the run is allowed to use. It also initializes other variables in the program. If the run is a restart of a previous experiment, IPT will input the momentum and position of each particle at the end of the last run, along with additional data necessary to continue the molecular dynamics calculations of the system.

IPT also contains entry points for outputing results at different points in time. OPT(0) prints out the initial state of the system such as, E_0, the total energy of the system, r_0, ρ_0, the position and momentum of each of the N particles in the system in terms of their components, and a graph of the velocity distribution, all at time t = 0. OPTM formats and outputs intermediate results at defined time intervals such as, t, the current time of the system, <s>, the mean nearest neighbor distance, T, the temperature of the system, P, the pressure of the system, ΔE and $\Delta\rho$, the change in the total energy and total linear momentum after the latest integration step, RKT and CLK, the amount of central processor time required for the last integration and the total central processor time used, and finally the number of occurences of each of the n-body collisions that occured during the latest integration step. Finally, OPT(1) is used to output the total energy, E_t, at the end of the run, the

final positions and momentum of the N particles, r_t and ρ_t, and a graph of the final velocity distribution. In addition OPT(1) outputs, either to cards or disk, all other data necessary to restart the experiment at a later time. IPT is illustrated in Figure 6.

INSET

INSET is used to establish the initial conditions of a computer experiment. The initial positions, r, and momentum, ρ, are selected from a random number table. The components of the position are then scaled such that every particle is within the confines of the box and at least 1.0σ away from any wall. Close collisions, that is, any particles closer than 0.9σ are separated to this distance. The total linear momentum is reduced to zero by subtracting 1/N times the total momentum from the momentum of each particle. The angular velocity of the system is found by applying the inverse of the inertia tensor to the total angular momentum. The angular momentum is reduced to zero by adding the negative of the angular velocity to the system as a whole. The linear momenta are then uniformly scaled to obtain the desired temperature. INSET is illustrated in Figure 7.

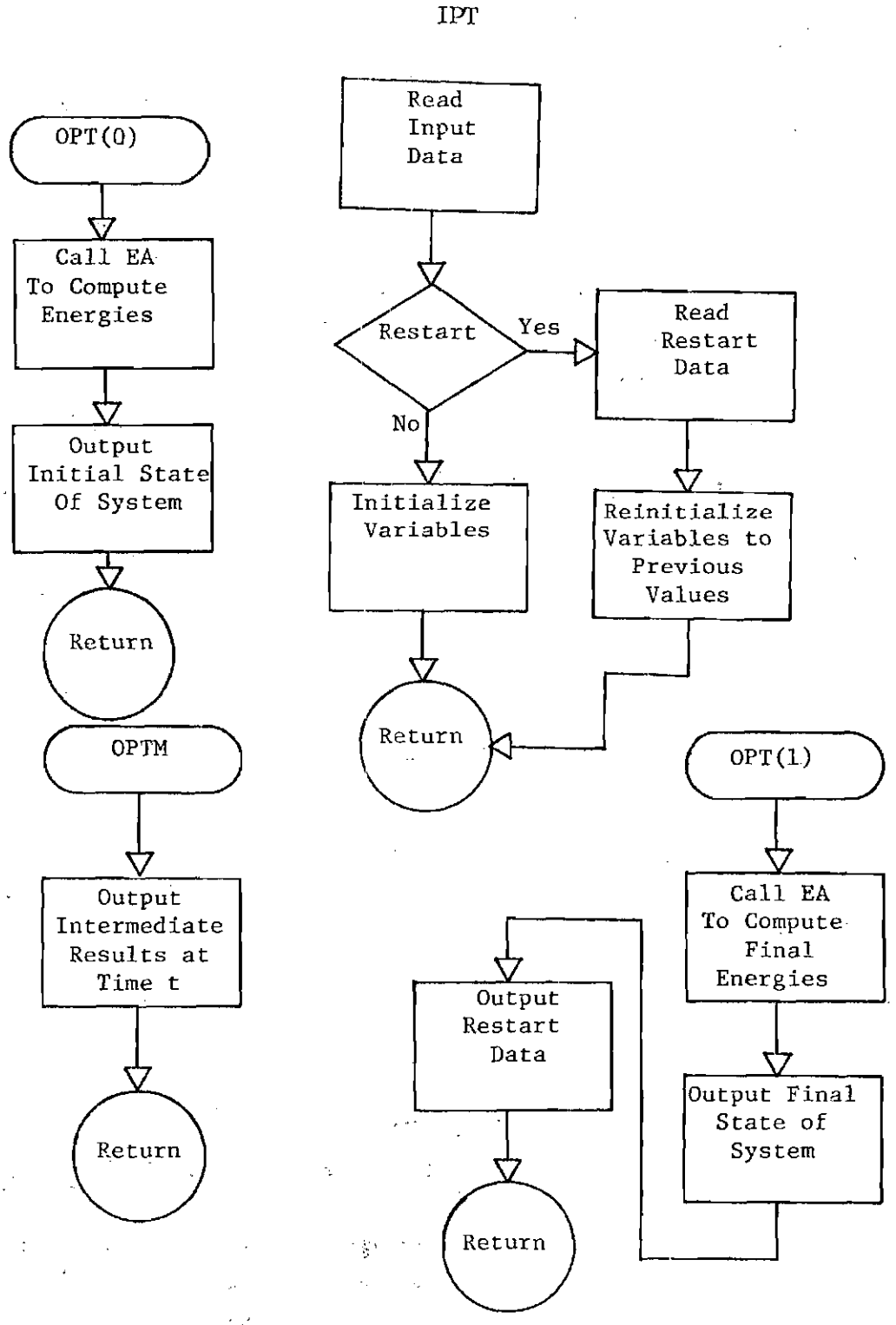

Figure 6. The Routine IPT.

INSET

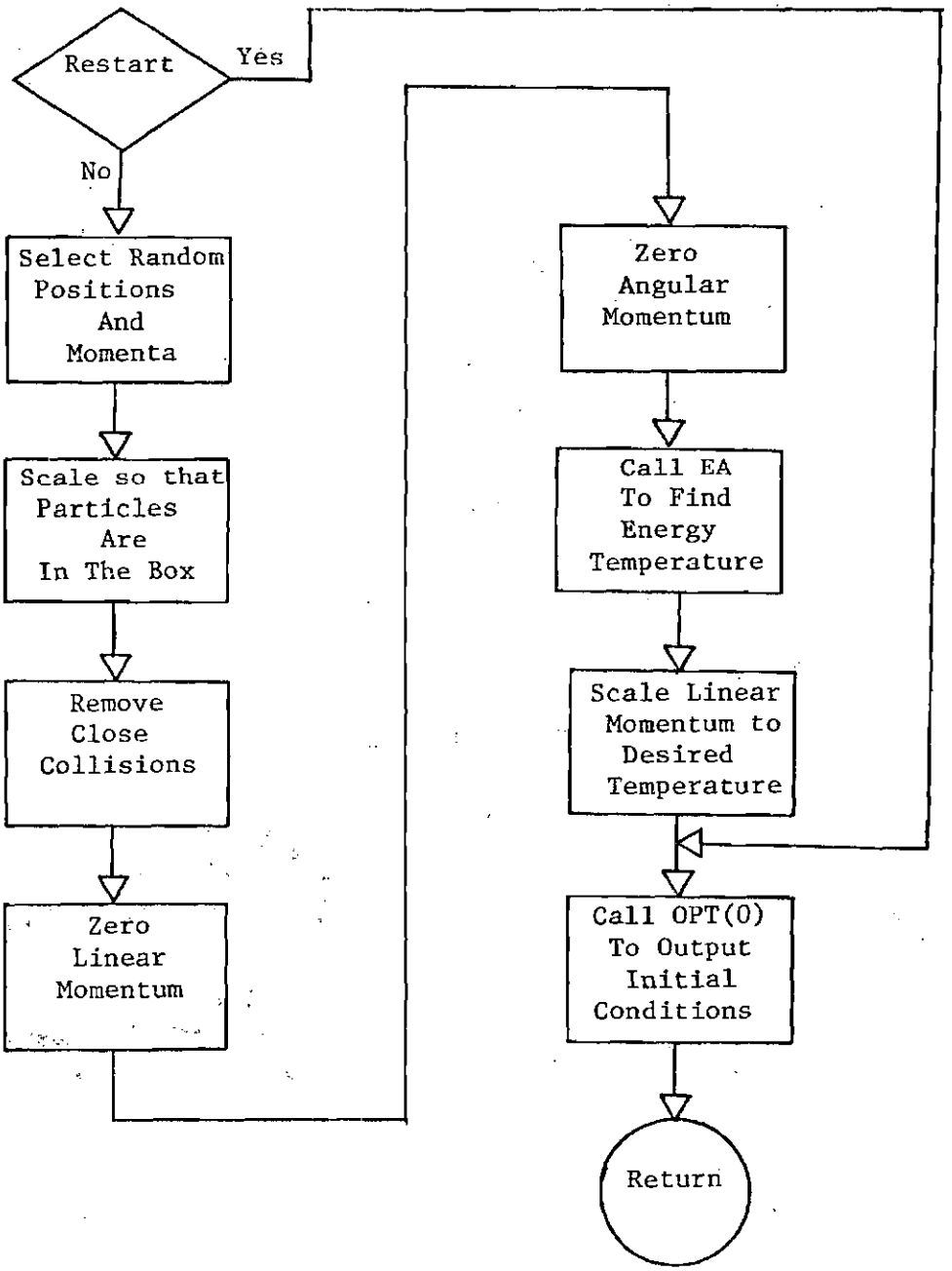

Figure 7. The Routine INSET.

EA

EA is a very simple routine designed to calculate the total kinetic energy of the system, K_t, the total potential energy, U_t, the total energy, E_t, and the temperature, T_t, at any time t. Figure 8 illustrates EA.

RK

RK is that procedure which performs the integration of the equations of motion to determine the positions and momenta of the N particles in the system at time $t+\Delta t$. RK contains the Runge-Kutta (39) method for the solution of the ordinary differential equations.

Given a second order, ordinary differential equation of the form

$$\frac{d^2y}{dx^2} = y'' = f(x,y,y') \qquad (19)$$

with initial conditions

$$x = x_o,\ y = y_o,\ \text{and}\ y' = y'_o$$

EA

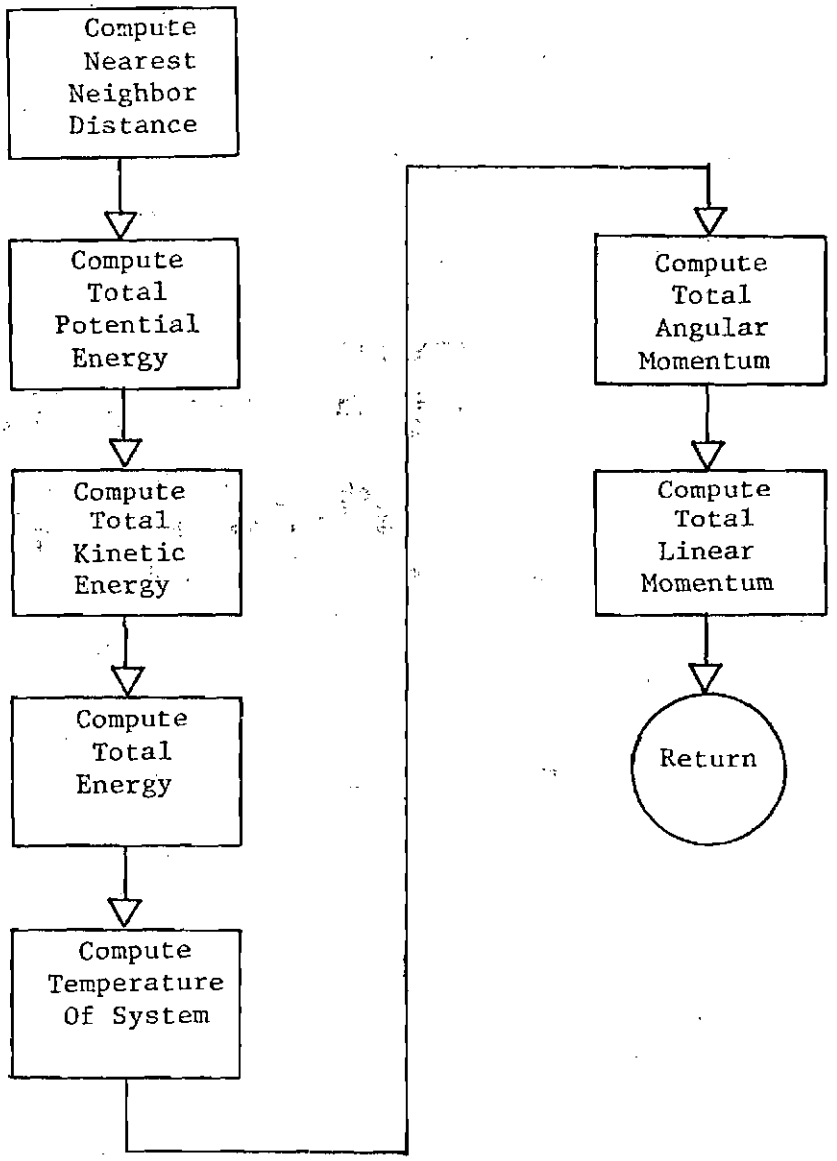

Figure 8. The Routine EA.

it is necessary to obtain

$$y'(x_o + h) \text{ and } y(x_o + h)$$

where h is an increment of the independent variable x.

The Runge-Kutta method is an algorithm which approximates the Taylor series solution. This numerical method does not require evaluations of derivatives beyond the first and is therefore self-starting, since only the functional values at a single previous point are required to obtain the functional values at the next point. In the fourth-order method, which was chosen for this research, four evaluations of the first derivative are required to obtain agreement with the Taylor series solution through terms of order h^4.

For a differential equation of the form of equation (19) the Runge-Kutta equations are

$$y_{n+1} = y_n + h[y'_n + \frac{1}{6}(k_1 + k_2 + k_3)] + O(h^5)$$

$$y'_{n+1} = y'_n + \frac{1}{6}(k_1 + 2k_2 + 2k_3 + k_4)$$

$$k_1 = hf(x_n,\ y_n + y_n')$$

$$k_2 = hf(x_n + \frac{1}{2}h,\ y_n + \frac{h}{2}y_n' + \frac{h}{8}k_1,\ y_n' + \frac{k_1}{2})$$

$$k_3 = hf(x_n + \frac{h}{2},\ y_n + \frac{h}{2}y_n' + \frac{h}{8}k_2,\ y_n' + \frac{k_2}{2})$$

and

$$k_4 = hf(x_n + h,\ y_n + hy_n' + \frac{h}{2}k_3,\ y_n' + k_3) \quad .$$

As was mentioned previously, one of the disadvantages of this method is the constant time increment, h, which must be chosen small enough for the integration procedure to yield new positions and momenta within an acceptable truncation error. Therefore, one of the design features of RK was the incorporation of a variable time increment.

In molecular dynamics calculations, the most time consuming portion of the program is the numerical integrations. The computer time required to determine new positions and momenta after a time interval, Δt, using the Runge-Kutta technique, depends on the number of equations that must be solved, on the step size, h, and on the potential function. Since one Runge-Kutta step will yield

the state of the system after a time step, h, the size of h determines how many integration steps are required to solve for the state of the system at time

$$t_2 = t_1 + \Delta t$$

where

$$\Delta t = nh, \; n = \text{integer} \quad .$$

Since each Runge-Kutta step requires a finite amount of central processor time, the larger the value of h that can be chosen and still maintain an acceptable truncation error, the smaller the amount of computer time required to solve the state of the system after a time interval, Δt. It is also true that the amount of computer time required to perform one integration step will depend on the number of equations to be solved, and therefore on the number of particles involved.

RK is an algorithm designed to take advantage of these two concepts in order to minimize the amount of central processor time required for the integration process. It is important initially to use a relatively large value of h, and if possible reduce the number of particles over which the integration must be performed. The basic notion of this algorithm is the concept of main and sub-integration steps.

A main integration step consists of integrating all 6N differential using a retatively large time step, h = Δt, generally chosen to be the print interval, that is, the interval of time after which OPTM will output intermediate results relative to the state of the system. After the main integration step is complete, the truncation error is computed for each of the N particles. There will be a group of M particles whose truncation error is within acceptable limits, and will require no further refinement of position or momentum by further integration. The N - M particles that are still in error are tabulated and put on a list. A sub-integration is then performed by reducing the size of the time step, h, and integrating the 6(N - M) differential equations. Truncation errors are then computed for the M particles, and another set of error particles are tabulated. The sub-integration process is repeated until the truncation error for all particles are within acceptable limits.

The complete RK algorithm can be described as follows:

Main integration step.

Set the number of integration steps NSTEP = 1.
Set the time step h = t, the print interval.
Integrate the 6N equations of motion for the new positions

and momentum

$$r_{t+\Delta t},\ \rho_{t+\Delta t} \quad .$$

Set the number of integration steps, NSTEP = 2(NSTEP).

Set the time step, h = h/NSTEP.

Perform NSTEP integrations of the 6N differential equations for

$$r^{*}_{t+\Delta t},\ \rho^{*}_{t+\Delta t} \quad .$$

Richardson (40) has shown that the truncation error in $r_{t+\Delta t}$ for a fourth-order Runga-Kutta integration is given by

$$\gamma = y - r \simeq \frac{|r^{*}_{t+\Delta t} - r_{t+\Delta t}|}{2^4 - 1} \qquad (20)$$

where Y denotes the true value of r at $t+\Delta t$. Equation (20) is based on the results of numerical integrations with steps of h and h/2, respectively.

Sub-integration step.

Given that γ^{*} is an acceptable truncation error in

position for the integration process, select all particles for which the following equation is true

$$\gamma^{*} - \gamma < 0 \quad . \tag{21}$$

If there are no particles for which equation (21) is true, then the new positions and momenta for the N particles have been accurately determined and RK is exited. Otherwise, those particles which are not in error, but which interacted with one or more error particles over the last sub-integration step must also be selected and put on the list. The sub-integration step is then repeated.

In addition to the integration performed by RK, the procedure sets up a disjoint circular list of all groups of particles of various orders (2-body, 3-body, ...) that occured during the integration process for later analysis by the routine CHIS for the purpose of counting n-body collisions. The RK algorithm is illustrated in Figure 9.

CHIS

The routine CHIS is called after the integration procedure is complete in order to count the number of n-body collisions that took place during the latest integration

RK

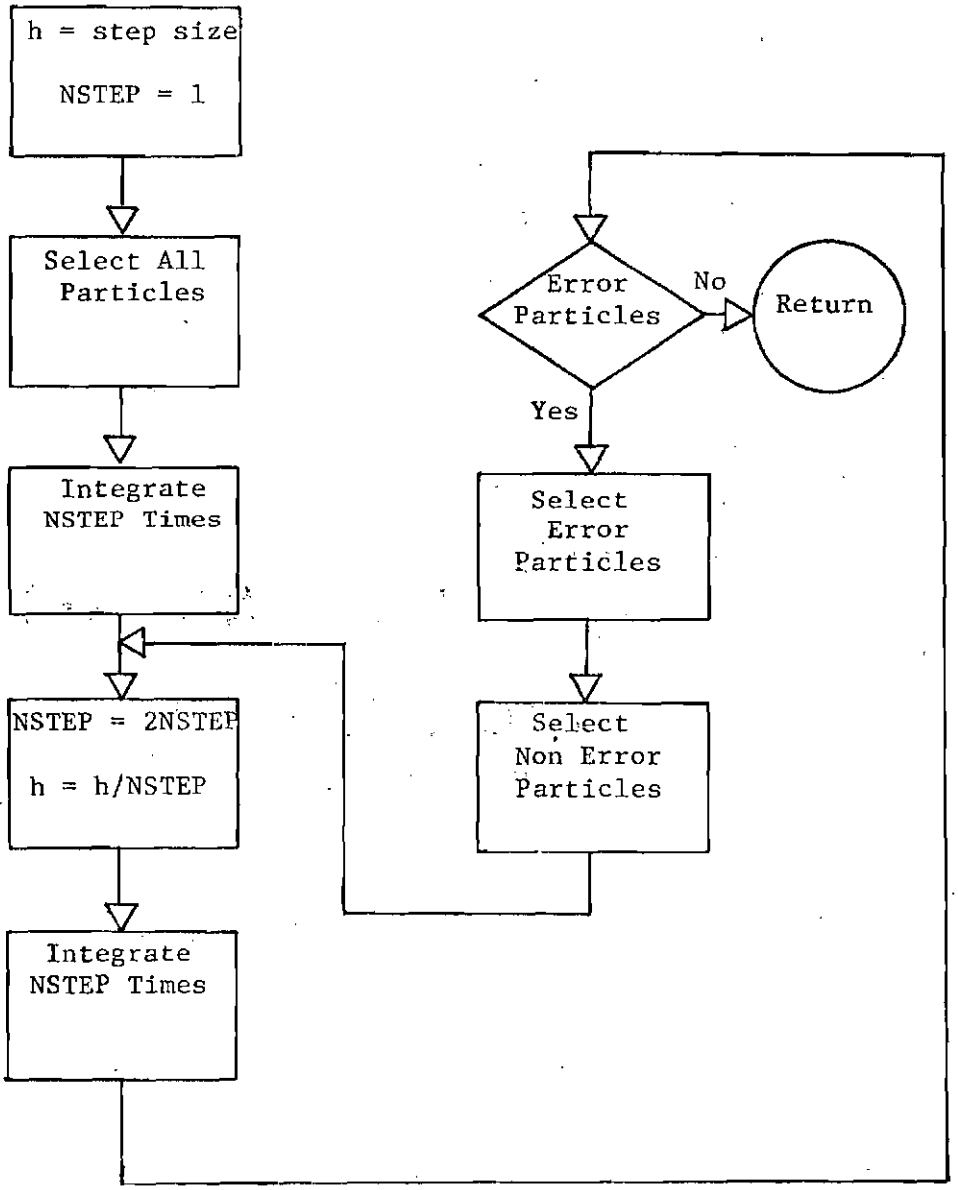

Figure 9. The Routine RK.

step. The Stoddard (38) definition of a collision is used.

An n-body collision is defined as the formation and subsequent dissolution of a group of n particles. A group is defined as a collection of particles such that each member of the group is within a given distance, C_r, of at least one other member. A collision is counted when the first particle leaves a group, but not when successive particles do, unless a new particle joins the group before the group becomes completely broken up. In this latter case a new collision is counted when the first particle leaves the new group.

The list L_i of circular chains is set up by RK during the integration process. Each list entry L_i represents the ith particle and contains a pointer to another member of the group containing particle i. If L_i points to itself, then the particle is not a member of any group. Figure 10 represents a group L_i of six particles of which particles one, two, and three form a 3-body group, particles five and six form a 2-body group, and particle four is a 1-body group.

CHIS compares the two group lists O_i and L_i where O_i represents the state of all groups in the system just before the latest integration of the system. L_i contains the group list after the latest integration. The four possible outcomes are illustrated in Figure 11.

i	1	2	3	4	5	6
L_i	3	1	2	4	6	5

Figure 10. A Circular List L_i.

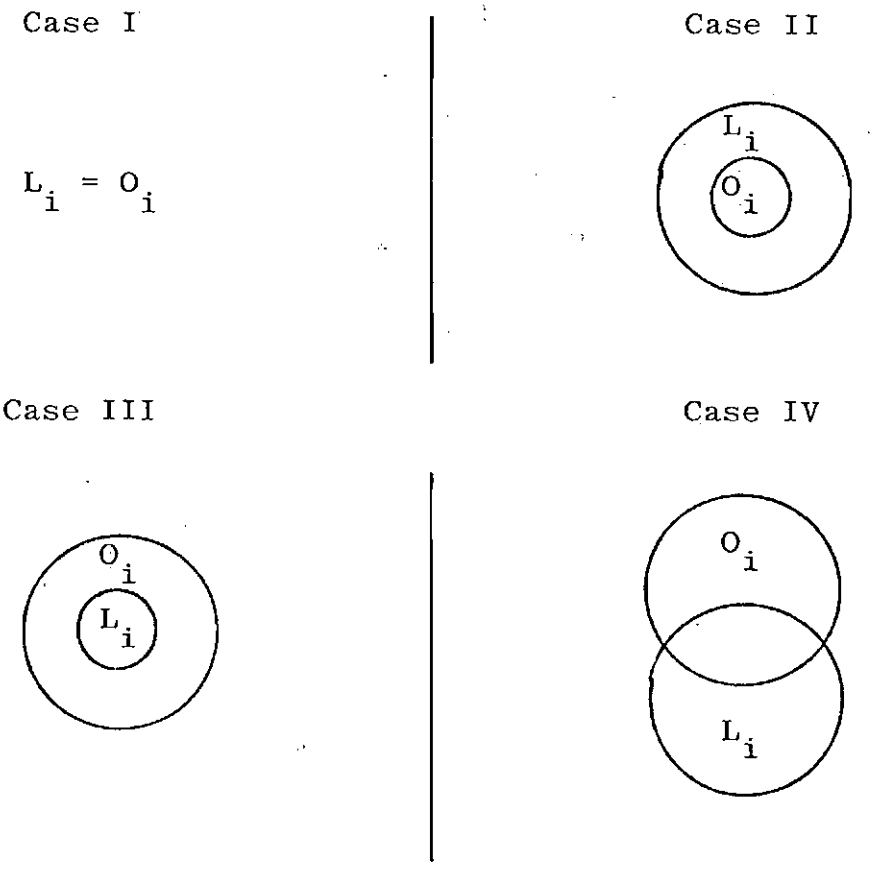

Figure 11. Possible Intersections of the O_i and the L_i Lists.

By comparing the two group lists L_i and O_i, the number of n-body collisions can be counted relative to the definition of a collision. For case I, O_i is identical to L_i, hence no particles have left any of the groups, and no collisions are possible. For case II, new groups have formed and have been added onto the L_i list, but again no particles have left any group in O_i, hence no collisions have occured. Cases III and IV both illustrate outcomes where collisions have occured. For the latter two cases, CHIS examines each group on the O_i list with groups on the L_i list which contain common particles, and determines the order of the collision. Finally the O_i list is replaced by the L_i list in preparation for the next call to RK. Figure 12 illustrates CHIS.

CHIS

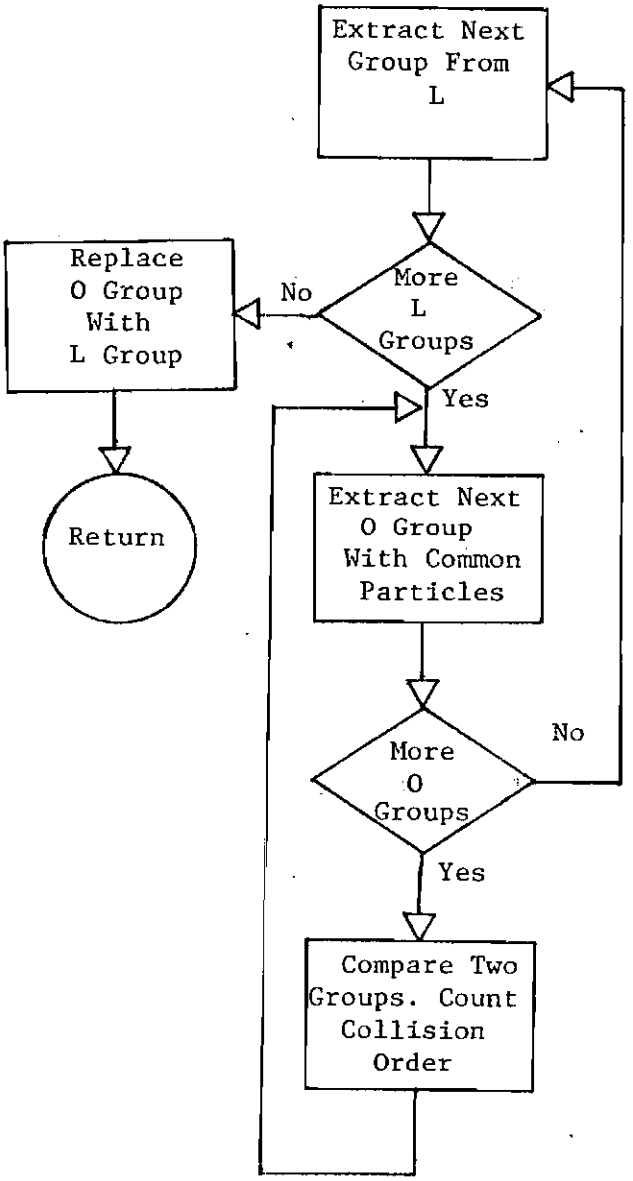

Figure 12. The Routine CHIS.

CHAPTER V

RESULTS AND CONCLUSIONS

In order to study the effect of a Lennard-Jones wall on a dilute monatomic Lennard-Jones gas, two groups of computer experiments were performed. The first group of experiments used the NOWALL model to calculate numerical quantities such as the temperature and pressure of a dilute gas in the absence of a wall. The second group of experiments used the WALL model to calculate the pressure and temperature of a dilute gas in the presence of a wall. In this manner, a comparison of the results allows the effect of the wall on the gaseous system to be determined.

The equation of state of the gaseous system was assumed to be a truncated form of the virial equation,

$$\frac{PV}{NkT} = 1 + B(T)\,\frac{N}{V} \tag{22}$$

The third, fourth, and higher order virial coefficients were assumed to be negligible compared to the second virial coefficient, B(T), since at low temperature, 2-body collisions would dominate, and there would be few, if any,

3-body and higher order collisions.

The second virial coefficient was the basis of comparison of the WALL and NOWALL models. For a two dimensional gas, which undergoes only 2-body collisions, a theoretical equation for the second virial coefficient may be derived for any pair potential function. The derivation of the two-dimensional formula for B(T) follows the same line of reasoning as the three-dimensional formula for B(T) given in Present (41). This two-dimensional equation is given by,

$$B(T) = \pi \int_0^\infty r[1 - e^{-U(r)/kT}]dr \qquad (23)$$

where U(r) is the pair interaction potential for the two-dimensional gas.

Equation (22) may be rearranged in the form

$$B(T) = \frac{PV^2}{N^2kT} - \frac{V}{N} \qquad (24)$$

Both the WALL and NOWALL models were designed to calculate the pressure and temperature of the system as a function of time. Using equation (24) the experimental second virial coefficient can be calculated for both the WALL and NOWALL

models and compared with the theoretical value of the second virial coefficient from equation (23).

Before any major computer experiments were performed, a number of preliminary experiments were designed to verify the accuracy of the computer programs. The NOWALL model was run for short periods of time to verify that the momentum change after collision with the walls was indeed 2mv for each particle. These runs also established that the cyclic boundary of the box was operating properly. Several runs for the WALL model were made at high temperatures, since at these temperatures the repulsive part of the potential function dominates, the particles behave very much like hard spheres, and the momentum change after interaction with the walls should be, and was observed to be 2mv for each particle. Both sets of experiments were carried out by placing single particles and multiple particles separated so they would not interact with each other in both the NOWALL and WALL box, and bouncing these particles against the walls.

Additional tests were performed by placing particles at known positions with known velocities so that certain multiple body collisions would occur. In this way, the collision counting section of the program was tested as well as the integration procedure of RK. Both sections were found to be performing correctly.

In addition to calculating and verifying numerical quantities, some of the early experiments were plotted so that the positions and velocities of the particles could be observed for short periods of time. One such plot is illustrated in Figure (13). The WALL model was used to calculate the positions and momenta of 20 two-dimensional particles in a square box, one side of which was 20 particle diameters long. The experiment was carried out at low temperature and high density to exaggerate the particle-particle interaction as well as the particle-wall interaction. The position of each particle is plotted as a circle of diameter 1.0σ as a function of time.

Figure (13) illustrates much of the characteristic behavior of such a system of gas particles. Notice the curvature of a particle's path as it is attracted by other particles or the wall. 2-body collisions can be observed to have taken place at various positions in the box with a resulting change in the momentum and direction of each of the colliding particles. In this particular run, 17 2-body and one 3-body collisions occured. Although it was felt that a particle which was adsorbed on the wall would tend to roll along the wall, Figure (13) indicates that in certain cases particles "hop" along the wall. In addition, because of the structure of the surface, the angle of incidence is often not

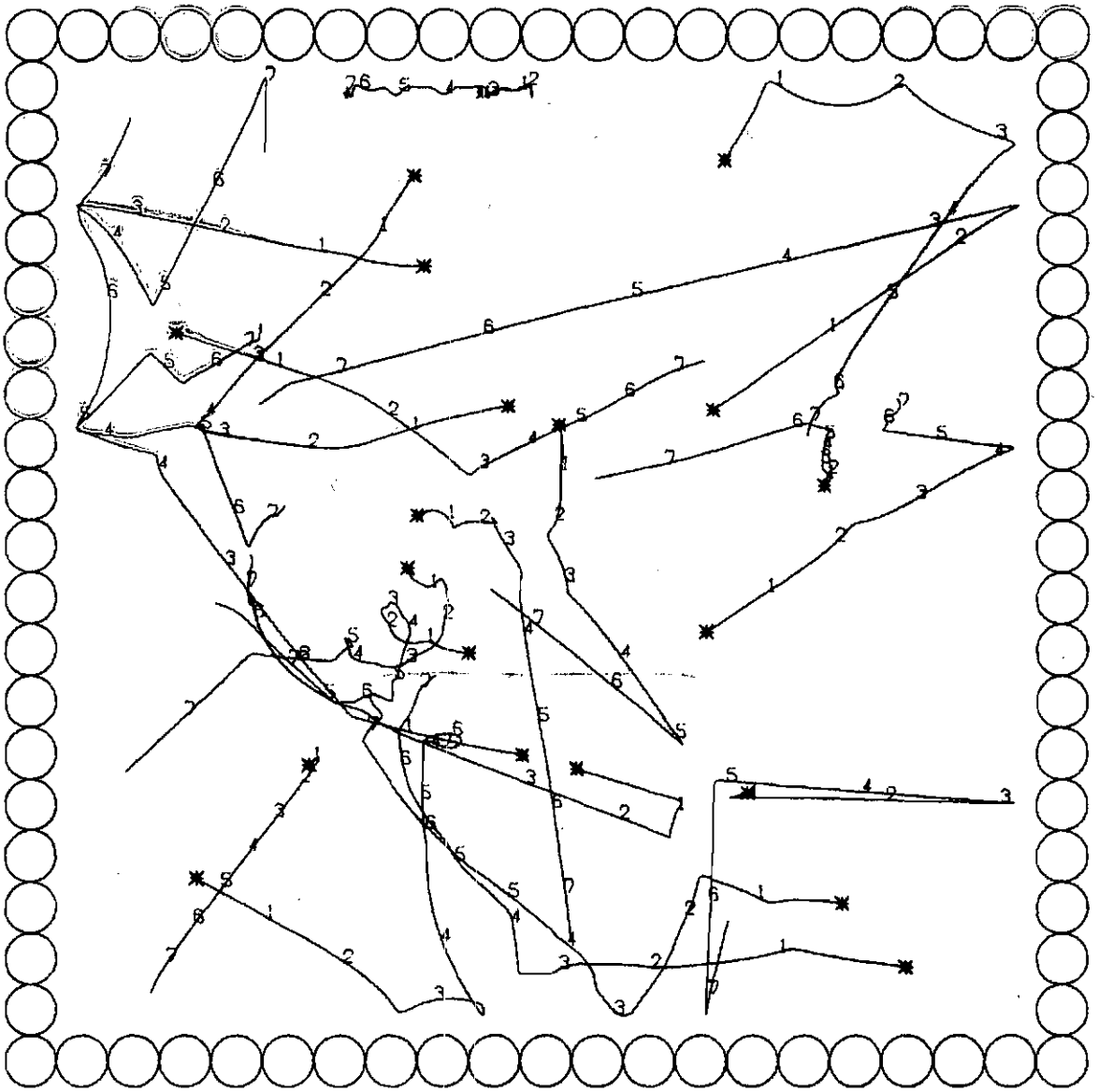

Figure 13. Plot of the Motion of 20 Particles Using the WALL Model.

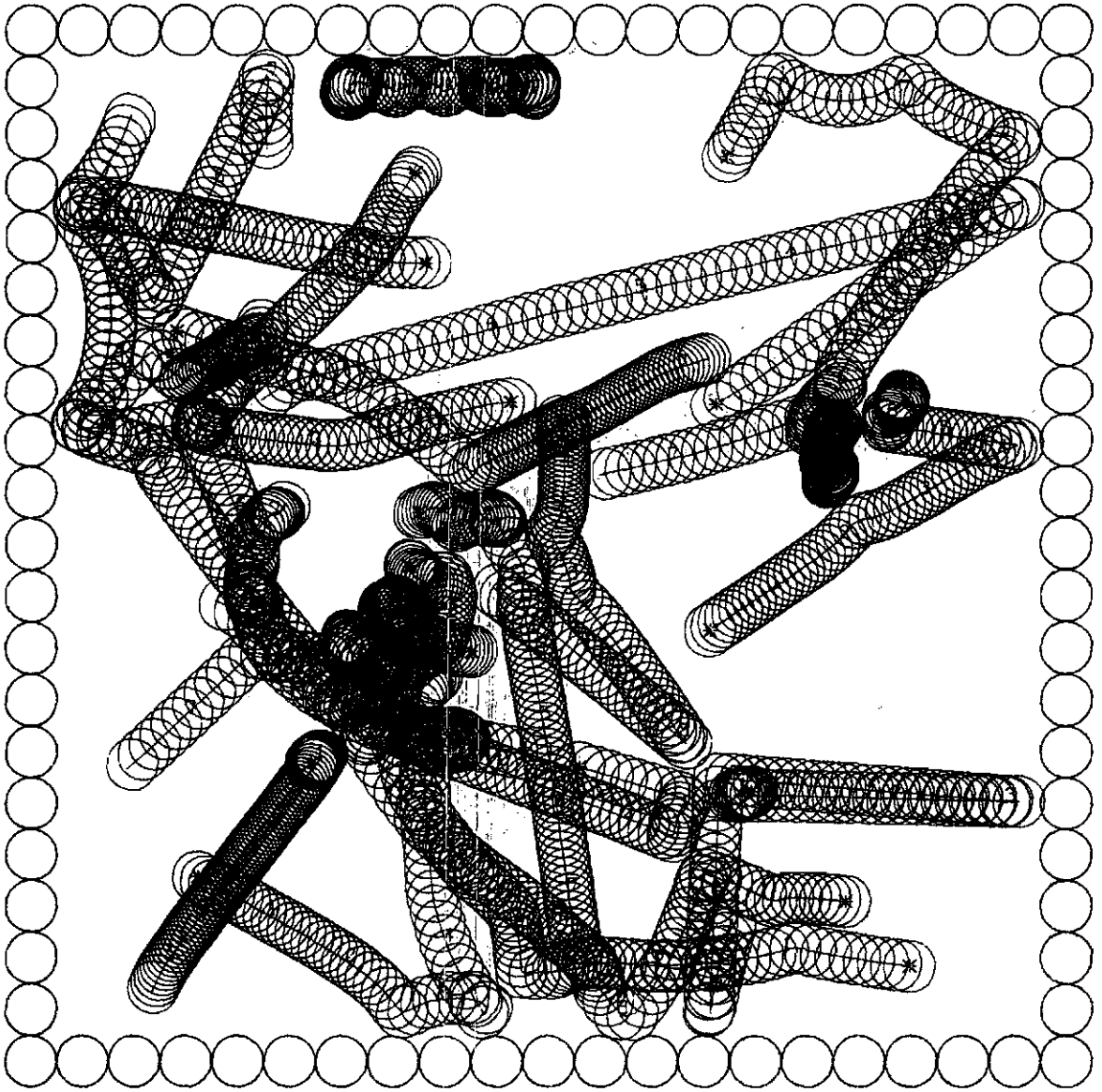

Figure 13A. Plot of the Motion of 20 Particles Using the WALL Model.

equal to the angle of reflection.

In the description of the computer experiments which follow, numerical quantities are reported in terms of reduced units unless otherwise stated. Table 1 gives the factors to convert from computer units to CGS units for a real gas. The Boltzmann constant is given by k; ε and σ are the Lennard-Jones parameters, and the abbreviations m.u., l.u., tm.u., e.u., and t.u. are for the computer units of mass, length, time, energy, and temperature respectively. Table 2 gives numerical conversion factors for various monatomic inert gases. The values of ε and σ were obtained from Hirschfelder (42).

Each experiment was conducted with N = 100 particles of diameter 1.0σ in a two-dimensional square box, one side of which was 150σ long. The range, r_c, of the interaction, equation (2), was defined to be $5.0\ \sigma$. The collision diameter, C_r (see Chapter IV, routine CHIS), was defined to be $1.0\ \sigma$. The truncation error of equation (20) was defined to be 1.0×10^{-5} for the purpose of determining the accuracy of the position and momentum of a particle after an integration step. The total energy of the system remains constant to 1.0×10^{-5} since the system is isolated. The initial momenta and positions of the 100 particles were

Table 1. Conversion Between Computer Units and CGS Units.

Quantity	Computer Units	Conversion Factor
Mass	1 m.u.	m
Length	1 l.u.	σ
Time	1 tm.u.	$\sigma(\frac{m}{4\varepsilon})^{1/2}$
Energy	1 e.u.	4ε
k (Boltzmann Constant)	1 $\frac{\text{e.u.}}{\text{t.u.-particle}}$	1.38×10^{-16} $\frac{\text{erg}}{^{o}\text{K-particle}}$
m (Particle Mass)	1 m.u.	m
σ	1 l.u.	σ
ε	1 e.u.	ε
Temperature	1 t.u.	$\frac{4\varepsilon}{k}$

Table 2. Numerical Conversion Factors Between Computer Units and CGS Units for Various Inert Monatomic Gases.

Quantity	Helium	Neon	Argon	Krypton	
Mass	6.65×10^{-14}	3.35×10^{-23}	6.63×10^{-23}	1.30×10^{-22}	g
Length	2.63×10^{-8}	2.78×10^{-8}	3.40×10^{-8}	3.60×10^{-8}	cm
Time	1.18×10^{-12}	1.16×10^{-12}	1.07×10^{-12}	1.40×10^{-12}	sec
Energy	3.33×10^{-15}	1.93×10^{-14}	6.72×10^{-14}	9.60×10^{-14}	erg
σ	2.63×10^{-8}	2.78×10^{-8}	3.40×10^{-8}	3.60×10^{-8}	cm
ε	8.32×10^{-16}	4.82×10^{-15}	1.68×10^{-14}	2.40×10^{-14}	erg
Temperature	2.41×10^{1}	1.40×10^{2}	4.88×10^{2}	6.84×10^{2}	^{o}K-particle

randomly selected, as described by routine INSET in Chapter IV.

Twelve experiments were performed using the NOWALL model with initial temperatures ranging from 0.1 to 7.0 computer units. Thirteen experiments were performed using the WALL model with initial temperatures ranging from 0.1 to 7.0 computer units. Each experiment was run until at least 200 2-body collisions had occured in order for the system to reach an approximate Maxwellian velocity distribution. The value of two collisions per particle for a system to reach equilibrium was reported by both Alder and Wainwright (3) and Harrison and Schieve (1).

The temperature and pressure of each experiment was tabulated every 0.1 time interval. Because the initial temperature of each system was near the equilibrium value, only small fluctuations in temperature occurred during the life of the experiment. The standard deviation of the instantaneous temperature, as calculated from step to step in the integration process, did not deviate from the tabulated time average by more than about 0.7% averaged over all NOWALL experiments, and about 2% averaged over all the WALL experiments. Therefore, the final temperature reported at the end of each computer experiment was taken to be the equilibrium temperature.

The pressure was very far from equilibrium initially. In addition, fluctuations in pressure were observed. These pressure fluctuations were due to the small number of particles in each system.

To obtain an equilibrium value of the pressure for each experiment, the following procedure was used. Plots of pressure versus time indicated that the pressure increased exponentially from the initial time and then leveled off to a constant value about which fluctuations occured. Therefore, a nonlinear least squares curve fitting program was used to fit the pressure data to the following equation

$$P(t) = C_1 + C_2 e^{-C_3 t} \tag{25}$$

where $P(t)$ is the pressure as a function of time t, and C_1, C_2, and C_3 are constants. Equation (25) is particularly advantageous, since at infinite time the pressure, P, is equal to C_1. This value was taken to be the equilibrium value of the pressure.

Because each experiment was run to different final times, the number of data points collected varied from experiment to experiment. In the case of very low

temperatures, this amounted to many thousands of data points. In order to reduce the computer time and memory necessary to curve fit the data, approximately 2000 data points were selected at evenly spaced time increments over the entire time interval of each run to be used in the curve fitting process. Initially, large fluctuations in pressure occurred as the pressure increased from zero as particles began colliding with the walls. In order to minimize the effect of these large initial fluctuations on the curve fitting process, the first 10% of the pressure data was weighted by the following formula,

$$W_i = \frac{i}{M}, \quad i \leq M$$
$$W_i = 1.0, \quad i > M \tag{26}$$

where W_i is the weight given to the ith point, and M is 10% of the total number of points selected.

In the nonlinear curve fitting process, the procedure was to chose values of the coefficients such that the residual sum of squares, RSS, was minimized. The residual sum of squares for L experimental data points is given by,

$$RSS = \sum_{i=1}^{L} W_i (P(t) - P_i)^2 \tag{27}$$

where P_i is the experimental pressure at the ith point, P(t) is the pressure calculated from equation (25) given values of C_1, C_2, and C_3 at the temperature t of the ith point, and W_i is the weighting factor given in equation (26). Additionally, the error in the pressure, ΔP, as calculated from the fitted data is given by,

$$\Delta P = \left(\frac{RSS}{L-1}\right)^{1/2} \tag{28}$$

This error is the standard deviation of the actual experimental values of P from the predicted values of P. It may be interpreted as an average error in predicting the pressure from equation (25).

Table 3 is a summary of each of the 12 experiments performed using the NOWALL model. The experiment number is given followed by the final time of the experiment, t_f, the temperature, T, the pressure, P, the residual sum of squares, RSS, the error in the pressure, ΔP, and the number of 2-body and 3-body collisions, 2B and 3B respectively. No 4-body or higher order collisions were ever observed. Table 4 summarizes the experiment number, the final time of the experiment, the temperature, the pressure, the residual sum of squares, the error in the pressure, and the number of 2-body and 3-body collisions for the 13 experiments using the

Table 3. Numerical Results of the 12 NOWALL Experiments in Computer Units.

Experiment Number	t_f	T	P	RSS	ΔP	2B	3B
1	792.5	.122	5.31×10^{-4}	7.04×10^{-7}	1.89×10^{-5}	250	0
2	713.7	.169	7.29×10^{-4}	1.59×10^{-6}	2.99×10^{-5}	250	0
3	684.1	.200	8.75×10^{-4}	1.81×10^{-6}	2.82×10^{-5}	250	0
4	497.1	.318	1.41×10^{-3}	2.33×10^{-5}	9.69×10^{-5}	250	1
5	440.1	.560	2.49×10^{-3}	2.55×10^{-5}	1.08×10^{-4}	250	0
6	3.44.4	.817	3.63×10^{-3}	4.68×10^{-5}	1.65×10^{-4}	250	0
7	306.1	1.05	4.83×10^{-3}	1.10×10^{-4}	2.68×10^{-4}	250	4
8	238.2	2.01	9.19×10^{-3}	5.43×10^{-4}	4.78×10^{-4}	250	1
9	160.0	4.00	1.78×10^{-2}	7.64×10^{-4}	6.92×10^{-4}	250	0
10	137.5	5.02	2.24×10^{-2}	9.41×10^{-4}	8.28×10^{-4}	250	0
11	129.8	6.00	2.68×10^{-2}	1.16×10^{-3}	9.46×10^{-4}	250	2
12	119.6	7.00	3.08×10^{-2}	3.17×10^{-3}	1.63×10^{-3}	250	1

Table 4. Numerical Results of the 13 WALL Experiments in Computer Units.

Experiment Number	t_f	T	P	RSS	ΔP	2B	3B
1	712.5	.118	4.35×10^{-4}	1.17×10^{-6}	2.57×10^{-5}	210	0
2	811.1	.140	5.49×10^{-4}	1.36×10^{-6}	2.59×10^{-5}	250	0
3	755.8	.160	6.76×10^{-4}	1.39×10^{-6}	2.71×10^{-5}	244	0
4	662.7	.212	9.01×10^{-4}	2.12×10^{-6}	3.10×10^{-5}	256	0
5	669.4	.308	1.32×10^{-3}	7.75×10^{-6}	5.90×10^{-5}	279	1
6	419.0	.502	2.22×10^{-3}	8.47×10^{-6}	6.44×10^{-5}	241	1
7	364.0	.839	3.80×10^{-3}	1.56×10^{-5}	9.26×10^{-5}	281	3
8	307.4	1.00	4.34×10^{-3}	1.83×10^{-5}	1.09×10^{-4}	258	0
9	253.9	2.00	8.84×10^{-3}	8.21×10^{-5}	1.80×10^{-4}	255	0
10	190.7	3.99	1.78×10^{-2}	1.27×10^{-4}	2.59×10^{-4}	305	2
11	151.3	5.01	2.20×10^{-2}	2.31×10^{-4}	3.91×10^{-4}	256	3
12	159.6	5.99	2.63×10^{-2}	3.07×10^{-4}	4.82×10^{-4}	277	1
13	134.9	7.03	3.06×10^{-2}	4.17×10^{-4}	5.56×10^{-4}	313	2

WALL model. Again, no 4-body or higher order collisions were observed. The error in the pressure, ΔP, in Table 3 as calculated from equation (28) ranges from 3.2% to 6.9% of P for the NOWALL experiments, and the error in the pressure in Table 4 ranges from 1.8% to 5.9% of P for the WALL experiments.

Given the pressure, P, temperature, T, volume, V, and number of particles, N, an experimental second virial coefficient can be calculated from equation (24) and compared to the theoretical second virial coefficient of equation (23). Table 5 gives the experiment number, temperature, T, experimental second virial coefficient, $B(t)_e$, and the theoretical second virial coefficient, $B(T)_t$, for the N = 100 particle systems using the NOWALL model. The temperature, experimental second virial coefficient and the theoretical second virial coefficient for the N = 100 particle systems using the WALL model is given in Table 6.

The data in Tables 5 and 6 are illustrated in Figure 14. The abscissa is logarithmic in temperature and the ordinate is linear in B(T). The theoretical second virial coefficient, equation (23), is plotted as a continuous line over the entire temperature range. The experimental second virial coefficients given in Table 5 for the NOWALL model are plotted as circles and the experimental second virial

Table 5. Numerical Values of the Theoretical and Experimental Second Virial Coefficient at Various Values of Temperature for the NOWALL Model.

Experiment Number	T	$B(T)_e$	$B(T)_t$
1	.122	-4.66	-6.26
2	.169	-6.62	-2.95
3	.200	-3.52	-1.96
4	.318	-0.531	-0.378
5	.560	0.100	0.487
6	.817	0.0689	0.777
7	1.05	7.88	0.899
8	2.01	6.46	1.06
9	4.00	0.281	1.10
10	5.02	0.896	1.09
11	6.00	1.13	1.08
12	7.00	-2.25	1.07

Table 6. Numerical Values of the Theoretical and Experimental Second Virial Coefficient at Various Values of Temperature for the WALL Model.

Experiment Number	T	$B(T)_e$	$B(T)_t$
1	.118	-38.4	-6.77
2	.140	-26.5	-4.56
3	.160	-11.1	-3.35
4	,212	-9.84	-1.68
5	.308	-8.04	-0.452
6	.502	-1.12	0.370
7	.839	4.29	0.792
8	1.00	-5.29	0.879
9	2.00	-1.24	1.06
10	3.99	0.846	1.10
11	5.01	-2.69	1.09
12	5.99	-2.72	1.08
13	7.03	-4.64	1.07

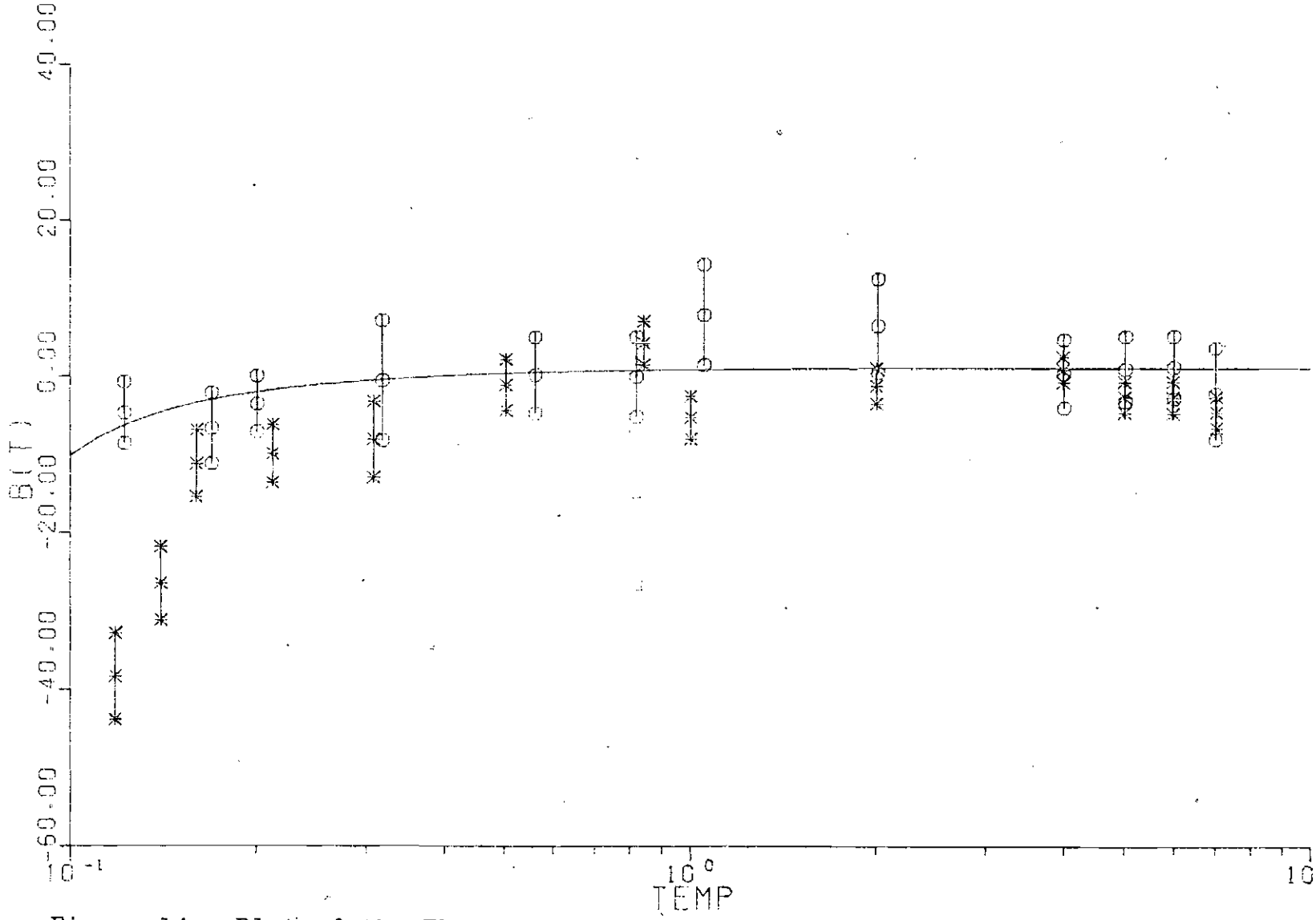

Figure 14. Plot of the Theoretical Second Virial Coefficients with the Experimental Second Virial Coefficients Calculated Using the WALL and NOWALL Models.

coefficients given in Table 6 for the WALL model are plotted as asterisks. Since the error in the pressure gives a corresponding error in the experimental $B(T)_e$, the experimental $B(T)_e$ data points in Figure 14 are plotted as a range of values where the center point in the range is the value of $B(T)_e$ from Tables 5 and 6.

A comparison of the experimental $B(T)_e$ for the NOWALL model with the theoretical $B(T)_t$ indicates that there is relatively good agreement over the entire temperature range as illustrated in Figure 14. Molecular modeling of a two-dimensional dilute gas of 100 particles using a computer model such as the NOWALL model, is a reasonable method of simulating a dilute gas in the absence of a wall.

In the presence of a wall, there is significant deviation of the experimental $B(T)_e$ when compared with the theoretical $B(T)_t$ at low temperature. Figure 14 clearly illustrates this deviation. At low temperature, the experimental $B(T)_e$ of the WALL model is lower than the theoretical value of $B(T)_t$. This negative deviation decreases as the temperature increases, and the experimental second virial coefficient appears to approach $B(T)_t$ somewhere in the temperature range of 0.7 to 0.9 computer units. Figure 14 also indicates that there may be a negative deviation of the experimental $B(T)_e$ at high temperature in

the range of 5.0 to 7.0 computer units, however, additional high temperature data points need to be calculated in order to verify that this deviation indeed exists.

The low temperature deviation of the experimental $B(T)_e$ is due to the interaction of the wall with the gas. This negative deviation is the result of a decrease in the pressure of the gaseous system which is assumed to be caused by the adsorption of particles on the wall. The difference between $B(T)_e$ and $B(T)_t$ may be used to calculate the number of particles that have been adsorbed.

Assuming N_a particles have been adsorbed, the theoretical $B(T)_t$ is equal to,

$$B(T)_t = \frac{PV^2}{(N - N_a)^2 kT} - \frac{V}{(N - N_a)} \quad . \qquad (29)$$

Given equation (24), equation (29) may be rearranged in the form,

$$\frac{B(T)_t}{N^2} N_a^2 + \left(\frac{-2B(T)_t N - V}{N^2}\right) N_a + B(T)_t - B(T)_e = 0 \quad . \qquad (30)$$

The quadratic formula may be used to solve equation (30) for the value of N_a.

The theoretical and experimental values of the second virial coefficient, given in Table 6, were used to calculate a value of N_a, from equation (30), for the first six low temperature WALL experiments. The four walls of the box contained 596 particles. The number of particles adsorbed divided by the number of wall particles is an indication of the amount of wall coverage by the adsorbed molecules. Table 7 gives the experiment number, reduced temperature, T, number of molecules adsorbed, N_a, and the coverage N_a/N_w, where N_w = 596 particles.

Pierotti and Thomas (43) have shown that for zero-coverage physical adsorption of a one component adsorbate, the second gas-solid virial coefficient, $B(T)_s$, is given by,

$$B(T)_s = \frac{N_a kT}{P} \tag{31}$$

and the enthalpy of adsorption, ΔH_{ads}, is given by,

$$\Delta H_{ads} = RT - q_{st} \tag{32}$$

where q_{st}, the isoteric heat of adsorption, is given by,

Table 7. Numerical Values for the Number of Particles Adsorbed and the Change in Enthalpy for Various Values of Temperature for the WALL Model.

Experiment Number	T	N_a	N_a/N_w
1	0.118	14.9	2.50×10^{-2}
2	0.140	10.1	1.69×10^{-2}
3	0.160	3.55	5.96×10^{-3}
4	0.212	3.68	6.17×10^{-3}
5	0.308	3.39	5.69×10^{-3}
6	0.502	0.660	1.11×10^{-3}

$$q_{st} = RT + R\left(\frac{d\ln B(T)_s}{d\left(\frac{1}{T}\right)}\right) \quad . \tag{33}$$

Substituting equation (33) into equation (32), the heat of adsorption at zero-coverage is then given by,

$$\Delta H_{ads} = -R\left(\frac{d\ln B(T)_s}{d\left(\frac{1}{T}\right)}\right) \quad . \tag{34}$$

Using values of N_a and T from Table 7 and the values of P from Table 4, values of $B(T)_s$ were calculated from equation (31) for the first six WALL experiments, and are given in Table 8. In order to evaluate a numerical quantity for ΔH_{ads}, equation (34), it is necessary to evaluate $d(\ln B(t)_s)/d(1/T)$. This was done by using a linear least squares curve fitting process to fit the values of $\ln B(T)_s$ versus 1/T from Table 8. The slope of the resulting straight line equals $d(\ln B(T)_s)/(d(1/T)$, which was found to be 0.431 computer units.

ΔH_{ads} was calculated for argon using the conversion factors from Table 2 and equation (34), and was found to be -418 calories per mole. Values of ΔH_{ads} for real monatomic inert gases are of the order of the ΔH_{vap}, which is generally a couple of thousand calories per mole. The value of ΔH_{ads}

Table 8. Numerical Values of the Temperature and the Second Gas-Solid Virial Coefficient in Computer Units.

Experiment Number	T	1/T	$B(T)_s$	ln $B(T)_s$
1	0.118	8.47	4.04×10^3	8.03
2	0.140	7.14	2.59×10^3	7.86
3	0.160	6.25	8.39×10^2	6.73
4	0.212	4.72	8.66×10^2	6.76
5	0.308	3.25	7.90×10^2	6.67
6	0.502	1.99	1.49×10^2	5.01

for argon calculated from the WALL experiments is about a factor of 10 smaller. This discrepancy is not surprising considering the limitations of the WALL model and the potential function between the wall and the gas particles. This result suggests several additional experiments which might be performed to determine what additional properties are important to more realistically model the adsorption of a real gas. For example, a different potential function could be used between the wall and the gas particles, a wall model could be designed to exchange energy with the particles in the gas, or the wall could be more accurately represented as a lattice several molecular layers deep instead of the monolayer that was used in the WALL experiments. Some of these new experiments will be performed in the near future.

The computer simulation of the classical dynamics of a dilute monatomic gas interacting through the Lennard-Jones 6-12 pair potential in the absence of a wall yields values of the second virial coefficient which approximate the values predicted by theory. The addition of a monomolecular Lennard-Jones wall indicates that the second virial coefficient deviates from the theoretical value at low temperature. This deviation indicates the adsorption of gas particles on the wall. Fluctuations in the calculation of the pressure may be reduced by an increase in the number of particles in the box, however, the CYBER 74-28 is not fast

enough to make the problem practical for a system of 1000 or more particles. In spite of this fact, it is important to note that the WALL model, using 100 particles, accurately predicts trends in numerical quantities, such as the negative deviation of the experimental second virial coefficient from the theoretical value.

BIBLIOGRAPHY

1. H. W. Harrison and W. C. Schieve, J. Stat. Phys. 3, 35 (1971).

2. B. J. Alder and T. E. Wainwright, J. Chem. Phys. 27, 1208 (1957).

3. B. J. Alder and T. E. Wainwright, Nuovo Cimento 9, Suppl. No. 1, 116 (1958).

4. B. J. Alder and T. E. Wainwright, J. Chem. Phys. 31, 459 (1959).

5. B. J. Alder and T. E. Wainwright, J. Chem. Phys. 33, 1439 (1960).

6. A. Rahman, Phys. Rev. 136(2A), 405 (1964).

7. B. J. Alder, Phys. Rev. Lett. 12, 317 (1964).

8. A. Rahman, Phys. Rev. Lett. 12, 575 (1964).

9. B. J. Alder, J. Chem. Phys. 40, 2742 (1964).

10. J. H. Dymond and B. J. Alder, J. Chem. Phys. 45, 2061 (1966).

11. B. J. Alder and T. E. Wainwright, Phys Rev. Lett. 18, 988, (1967).

12. B. J. Alder, D. M. Gass, and T. E. Wainwright, J. Chem. Phys. 53, 3813 (1970).

13. L. Verlet, Phys. Rev. 159, 98 (1967).

14. L. Verlet, Phase Transitions, Proc. Conf. Chem. 14th (1969), pub. 1971, pp. 65-103.

15. L. Verlet, Physikertag. Vorabdrucke Kurzfassungen Farber., 35th 1970, N7-N11.

16. R. E. Allen, F. W. DeWette, and A. Rahman, Phys. Rev. 179, 887 (1969).

17. R. E. Allen and F. W. DeWette, Phys. Rev. 179, 873 (1969).

18. F. W. DeWette, R. E. Allen, D. S. Hughes, and A. Rahman, Phys. Lett. 29A, 548 (1969).

19. A. Rahman, Rivista Nuovo Cimento 1, 315 (1969).

20. H. W. Harrison, W. C. Schieve, and J. S. Turner, J. Chem. Phys. 56, 710 (1972).

21. H. W. Harrison and W. C. Schieve, J. Chem. Phys. 58, 3634 (1973).

22. B. Borstnik and A. Azman, Ber. Bunsenges. Phys. Chem. 75(3/4), 392 (1971).

23. C. H. Bennett and B. J. Alder, J. Phys. and Chem. Solids 32, 2111 (1971).

24. D. M. Gass, B. J. Alder, and T. E. Wainwright, J. Phys. and Chem. Solids 32, 1797 (1971).

25. B. J. Alder, D. A. Young, and M. A. Mark, J. Chem. Phys. 56, 3013 (1972).

26. P. T. Herman and B. J. Alder, J. Chem. Phys. 56, 987 (1972).

27. B. J. Alder, Comput. Phys. Commun. 3(suppl.), 86 (1972).

28. A. Rahman and F. H. Stillinger, J. Chem. Phys. 55, 3336 (1971).

29. F. A. Stillinger and A. Rahman, J. Chem. Phys. 57, 1282 (1972).

30. A. Rahman and F. A. Stillinger, Conference on Molecular Motion in Liquids and 24th Annual Meeting of the Society of Physical Chemistry, Orsay, France, 2-6 July 1973 (Paris France: Soc. Phys. Chem. 1973) pp. 45/1-2.

31. B. J. Alder, Phys. Rev. 7A, 281 (1973).

32. B. J. Alder, H. L. Strauss, and J. J. Weis, J. Chem. Phys. 59, 1002 (1973).

33. B. J. Berne, M. Bishop, and A. Rahman, J. Chem. Phys. 58, 2696 (1973).

34. G. Subramanian, D. Levitt, and H. T. Davis, J. Chem. Phys. 60, 591 (1974).

35. P. Schofield, Comput. Phys. Commun. 5, 17 (1973).

36. B. J. Alder, Annual Reviews of Physical Chemistry, edited by H. Erying, p. 325, Annual Reviews Inc., Palo Alto, Calif., 1973.

37. A. Aharony, J. Comput. Phys. 10(2), 341 (1972).

38. S. D. Stoddard, Jr., Doctorial Dissertation, Georgia Institute of Technology, 1973.

39. M. Abramowitz and I. A. Stegun, eds., Handbook of Mathematical Functions with Formulas, Graphs, and Mathematical Tables, p. 897, U. S. Department of Commerce National Bureau of Standards, U. S. Government Office, Washington, D. C., 1965.

40. L. F. Richardson and J. A. Gaunt, Trans. Roy. Soc. London 226A, 300 (1927).

41. R. D. Present, Kinetic Theory of Gases, pp. 103-107, McGraw-Hill Book Company, New York, 1958.

42. J. O. Hirschfelder, C. F. Curtiss, and R. B. Bird, Molecular Theory of Gases and Liquids, p. 1110, John Wiley and Sons, New York, 1954.

43. R. A. Pierotti and H. E. Thomas, Surface and Colloid Science Vol. 4, edited by Egon Matijevic, p. 93, Wiley Interscience, New York, 1971.